

## PUBLISHED VERSION

Paton, Fiona Laura; Maier, Holger R.; Dandy, Graeme Clyde  
Relative magnitudes of sources of uncertainty in assessing climate change impacts on water supply security for the southern Adelaide water supply system, *Water Resources Research*, 2013; 49(3):1643-1667.

Copyright 2013. American Geophysical Union. All Rights Reserved.

### PERMISSIONS

<http://publications.agu.org/author-resource-center/usage-permissions/>

#### **Permission to Deposit an Article in an Institutional Repository**

Adopted by Council 13 December 2009

AGU allows authors to deposit their journal articles if the version is the final published citable version of record, the AGU copyright statement is clearly visible on the posting, and the posting is made 6 months after official publication by the AGU.

**8<sup>th</sup> October 2013**

<http://hdl.handle.net/2440/79466>

## Relative magnitudes of sources of uncertainty in assessing climate change impacts on water supply security for the southern Adelaide water supply system

F. L. Paton,<sup>1</sup> H. R. Maier,<sup>1</sup> and G. C. Dandy<sup>1</sup>

Received 14 May 2012; revised 12 February 2013; accepted 15 February 2013; published 28 March 2013.

[1] The sources of uncertainty in projecting the impacts of climate change on runoff are increasingly well recognized; however, translating these uncertainties to urban water security has received less attention in the literature. Furthermore, runoff cannot be used as a surrogate for water supply security when studying the impacts of climate change due to the nonlinear transformations in modeling water supply and the effects of additional uncertainties, such as demand. Consequently, this study presents a scenario-based sensitivity analysis to qualitatively rank the relative contributions of major sources of uncertainty in projecting the impacts of climate change on water supply security through time. This can then be used by water authorities to guide water planning and management decisions. The southern system of Adelaide, South Australia, is used to illustrate the methodology for which water supply system reliability is examined across six greenhouse gas (GHG) emissions scenarios, seven general circulation models, six demand projections, and 1000 stochastic rainfall time series. Results indicate the order of the relative contributions of uncertainty changes through time; however, demand is always the greatest source of uncertainty and GHG emissions scenarios the least. In general, reliability decreases over the planning horizon, illustrating the need for additional water sources or demand mitigation, while increasing uncertainty with time suggests flexible management is required to ensure future supply security with minimum regret.

**Citation:** Paton, F. L., H. R. Maier, and G. C. Dandy (2013), Relative magnitudes of sources of uncertainty in assessing climate change impacts on water supply security for the southern Adelaide water supply system, *Water Resour. Res.*, 49, 1643–1667, doi:10.1002/wrcr.20153.

### 1. Introduction

[2] Water supply systems in the developed world have previously been planned and managed assuming that natural systems, although exhibiting fluctuations, operate in an unchanging envelope of variability [Milly *et al.*, 2008]. However, as pointed out by Milly *et al.* [2008], this assumption of stationarity is dead because of the impacts of substantial anthropogenic global warming on the hydrologic cycle. Thus, using historic climate to plan and manage future water supply systems is no longer valid; instead, projections of future climate should be used to guide decision making. However, there still exist large uncertainties in projecting future climate and in understanding how these projections translate to water resources, such as runoff or water supply. Consequently, water resource planners must understand the greatest sources of uncertainty, so as to be able to undertake

the difficult task of implementing robust management policies in an uncertain environment [Salas *et al.*, 2012].

[3] Chen *et al.* [2011b] developed the following cascade of the sources of uncertainty when determining climate change impacts on hydrology: (1) greenhouse gas (GHG) emissions scenarios, (2) general circulation model (GCM) structures and parameters, (3) GCM initial conditions, (4) downscaling methods, (5) hydrological model structures, and (6) hydrological model parameters. A brief description of the sources of uncertainty in this cascade is given below.

[4] In 2000, the Intergovernmental Panel on Climate Change (IPCC) published the “Special Report on Emissions Scenarios” (SRES) [Intergovernmental Panel on Climate Change, 2000], in which GHG emissions scenarios (labeled SRES scenarios) were defined. These reflect different world development pathways based on demographic, economic, and technological drivers [Intergovernmental Panel on Climate Change, 2007]. For the various SRES scenarios, GCMs are the best tools available for simulating climate at global and regional scales [Mpelasoka and Chiew, 2009]; however, the modeling uncertainty associated with GCMs contributes to the total uncertainty of the future climate. Although there is considerable confidence in GCMs to provide credible, quantitative future climate projections, particularly at the continental scale or greater, the models do differ considerably in terms of estimating

<sup>1</sup>School of Civil, Environmental and Mining Engineering, University of Adelaide, Adelaide, Australia.

Corresponding author: F. L. Paton, School of Civil, Environmental and Mining Engineering, University of Adelaide, Adelaide 5005, Australia. (fpaton@civeng.adelaide.edu.au)

the strength of different feedbacks in the climate system [Randall et al., 2007]. Consequently, the projections of future climate variables differ between GCMs, and this is more pronounced for certain variables, such as precipitation [Randall et al., 2007]. Furthermore, initial conditions of a GCM run can alter the output, reflecting natural variability of the climate system [Cubasch et al., 2001]. It is important to note that while this discussion relates to the set of coordinated climate model experiments comprising the World Climate Research Programme's Coupled Model Intercomparison Project CMIP3, a new set of simulations (CMIP5) are currently being developed.

[5] Additional uncertainty is introduced when the coarse-scale resolution variables produced by GCMs are down-scaled to a finer spatial scale; one that is suitable for modeling the impacts of climate change on catchment runoff. The first major method to do this is statistical downscaling, which uses statistical methods to establish empirical relationships between GCM outputs and local climate variables [Fowler et al., 2007]. Dynamical downscaling, the other major method, achieves fine scale variables by embedding a higher-resolution climate model within a GCM [Fowler et al., 2007]. An overview of these downscaling methods is presented by Fowler et al. [2007], which includes a comparison of the methods, including their merits and caveats. Hydrological modeling also causes uncertainty in projecting climate change impacts. For example, there are a myriad of rainfall-runoff (RRO) models that are used to translate local-scale climate variables, such as precipitation and evaporation, to runoff projections. The various RRO models use different climate inputs, different model parameters, run at different time steps and must be calibrated.

[6] In terms of the impact of climate change on future runoff, there has been increasing attention given to uncertainties in GHG emissions scenarios, GCM models, GCM initial conditions, downscaling techniques, and hydrological models and parameters [Boé et al., 2009; Chen et al., 2011a, 2011b; Chiew and McMahon, 2002; Chiew et al., 2009b, 2009c, 2010; Diaz-Nieto and Wilby, 2005; Dibike and Coulibaly, 2005; Forbes et al., 2011; Majone et al., 2012; Manning et al., 2009; Mpelasoka and Chiew, 2009; Wilby and Harris, 2006; Wilby et al., 2006]. A number of these studies have also explicitly compared the magnitude of runoff changes caused by the different sources of uncertainty associated with climate change and hydrological modeling [Boé et al., 2009; Chen et al., 2011a, 2011b; Chiew et al., 2009c; Mpelasoka and Chiew, 2009; Wilby and Harris, 2006]. The most comprehensive comparison by Chen et al. [2011b] assessed the overall uncertainty of hydrological impacts of climate change for a Canadian watershed, by examining six GCMs, five GCM initial conditions, two GHG emissions scenarios, four statistical downscaling techniques, three hydrological model structures, and 10 sets of hydrological model parameters. For mean annual discharge, the study concluded the following order of uncertainty source significance (from greatest to least): GCM > GCM initial conditions > GHG emissions scenario > statistical downscaling technique > hydrological model > hydrological model parameters.

[7] While in many cases runoff is a good indicator of water availability, the impacts of climate change on runoff do not necessarily correlate with those on water supply. For

example, Zhu et al. [2005] discovered that in California most climate change scenarios with increased precipitation resulted in less available water because of the seasonal rainfall pattern and storage capacities; that is, less summer runoff was not compensated by more winter runoff, because the storages could not accommodate increased winter flows. Water supply systems also have additional complexities in comparison to runoff. These include the uncertainties associated with future population, per capita water demand, regulatory requirements, water law, consumer preferences, and environmental standards [Wiley and Palmer, 2008]. Furthermore, model complexity is enhanced when modeling climate change impacts on water supply because not only do water simulation models incorporate demand, but they can also model (1) water storages, (2) transmission systems, (3) treatment systems, and (4) user-specified operating rules [Traynham et al., 2011]. Consequently, because of the additional complexity and uncertainty when moving from analyzing runoff to water supply, it cannot be assumed that the magnitude of uncertainties of climate change impacts on runoff equal that for water supply.

[8] A number of studies have examined the impact of climate change on water supply systems [Fowler et al., 2003; Gober et al., 2010; Groves et al., 2008; Kaczmarek et al., 1996; Lopez et al., 2009; O'Hara and Georgakakos, 2008; Traynham et al., 2011; Vicuna et al., 2010; Wiley and Palmer, 2008; Zhu et al., 2005], with most of these studies developing projected ranges of water availability based on a number of different uncertainties. For example, Wiley and Palmer [2008] examined uncertainty of GCMs, O'Hara and Georgakakos [2008] analyzed uncertainty of GCMs and population growth, Vicuna et al. [2010] examined uncertainty of GCMs and GHG emissions scenarios, while Gober et al. [2010] investigated the uncertainty of GCMs, GHG emissions scenarios, runoff factors, supply and demand management policies, and population growth. However, none of the studies compared the uncertainty sources in terms of their relative magnitudes. This is important because water authorities must understand the greatest sources of uncertainties for water supply system security and whether these are epistemic (systematic) or aleatoric (statistical). Systematic uncertainties, such as model inadequacy or data measurement inaccuracies, are potentially reducible (by the water authority's means or others), whereas statistical uncertainties, such as natural rainfall variability, are inherent and will always exist. If major sources of uncertainty are reducible by the water authority, then effort can be directed toward reducing this uncertainty, while if irreducible uncertainties dominate impacts on water supply security, then adaptation responses must be developed to cope with this uncertainty. Furthermore, an understanding of how these uncertainties interact through the development of "best" and "worst" cases will help water authorities establish likely bounds of future water supply security, which is imperative for them to understand the degree to which water supply may need to be supplemented, or demand reduced, in the future. In order to understand the impacts of uncertainties associated with modeling the likely impacts of climate change on water supply security, a number of approaches can be applied. A "top-down" or "scenario-based" approach, in which

uncertainty is added at each point of the modeling process from GHG emissions scenarios through to water supply system models, is the most commonly used approach within scientific evidence reviewed by the IPCC [Wilby and Dessai, 2010], and is the approach applied in the current paper. However, as discussed by Wilby and Dessai [2010], “bottom-up” and “sensitivity-based” approaches can also be applied to analyze uncertainties surrounding the likely impacts of climate change on water supply systems.

[9] When examining the impacts of climate change on water supply systems, it is also important to consider the temporal aspects of water supply security. Due to the large-scale infrastructure associated with water supply systems and the potentially long lead times for expanding these systems, it is necessary to identify when water supply security will be jeopardized in the future, so that plans to avoid water scarcity can be implemented well in advance. With the many uncertainties associated with analyzing the impacts of climate change on water supply security, it would be prudent to assume that the estimated point in time when water security is threatened will vary considerably depending on the choices made in modeling climate change, hydrology, and the water supply system. Consequently, monitoring how water supply security will change progressively through time at regular intervals over a long-term planning horizon of 30–50 years is very important. This is quite different to analyzing the impacts of climate change on runoff because in the case of water supply security, the addition of demand means a “failure” of supply to meet demand can be identified at a critical point in time, while there are no such critical points when examining runoff.

[10] In summary, there still exists a gap in understanding the relative magnitudes of uncertainty sources in assessing the impacts of climate change on water supply systems that can help water authorities plan for, and manage, the impacts of climate change. A scenario-based sensitivity analysis has therefore been developed and applied to Adelaide’s southern water supply system that focuses on the three objectives of this paper: (i) to assess the relative magnitudes of the major sources of uncertainty, (ii) to identify critical points in the future when water supply security is likely to be threatened, and (iii) to present projected ranges of water supply security. The results obtained from addressing these objectives are used to draw conclusions about the planning and management of Adelaide’s southern water supply system. While the methodology is illustrated for this particular case study, its generic nature means it could easily be adapted and applied to other water supply systems around the world.

[11] The remainder of the paper is organized as follows. First, the Adelaide southern system case study is introduced (section 2), followed by the methodology applied to meet the three objectives of this paper (section 3). The results of the case study are then presented and discussed (section 4), before the main components of the paper are summarized and conclusions are drawn (section 5).

## 2. Case Study

[12] Adelaide, the capital of South Australia (Figure 1), is the driest Australian capital city with an average annual

rainfall of 552 mm. Adelaide’s rainfall is strongly seasonal, falling predominantly during mild winters, which are separated by dry, hot summers. Adelaide also experiences high interannual variability, with a minimum recorded annual rainfall of 274 mm and a maximum of 883 mm (for Kent Town, Adelaide: 1889–2010 [Jeffrey et al., 2001]). Furthermore, there is high interdecadal variability in Adelaide. For example, the 1920s were 13% wetter than the long-term average, while the 1960s were 9% drier (for Kent Town, Adelaide [Jeffrey et al., 2011]).

[13] Historically, water has been sourced from reservoirs in nearby catchments in the Mount Lofty Ranges. These storages can hold a total of approximately 200 GL of water, equivalent to a little more than one year’s water supply for Adelaide. In most years, water from the River Murray is pumped about 50–60 km to supplement Adelaide’s water supply.

[14] This study focuses on Adelaide’s southern system of reservoirs, namely Myponga, Mount Bold, and Happy Valley. The southern system, which supplies approximately half of Adelaide’s demand, can be considered separately from Adelaide’s northern system of reservoirs because the two systems largely act independently of each other [Crawley and Dandy, 1993].

[15] Myponga Reservoir in the South (Figure 1) has a capacity of 26.8 GL and is a “supply and storage” reservoir, with water collected from its 124 km<sup>2</sup> catchment (Figure 1), before being treated at Myponga Water Treatment Plant (WTP), which has a capacity of 50 ML/day (see www.sawater.com.au). Mount Bold Reservoir has a much larger catchment and storage capacity (Figure 1)—388 km<sup>2</sup> and 46.2 GL, respectively (see www.sawater.com.au)—but is considered a “storage” reservoir because it cannot directly supply water to the water distribution network. Instead, water is released from Mount Bold Reservoir and diverted 6 km downstream at Clarendon Weir via the Horndale Flume to Happy Valley Reservoir (Figure 1) [Teoh, 2002]. Clarendon Weir is a small reservoir with a capacity of 0.3 GL, while Happy Valley Reservoir has a capacity of 11.6 GL (see www.sawater.com.au). Happy Valley Reservoir is considered an “off-stream” reservoir, with water only being supplied via the Horndale Flume, while Clarendon Weir receives water released from Mount Bold Reservoir, as well as runoff from its 54 km<sup>2</sup> catchment (Figure 1). The main purpose of Happy Valley Reservoir is to store water prior to treatment at the Happy Valley WTP, which has a capacity of 850 ML/day (see www.sawater.com.au).

[16] Mount Bold Reservoir also receives water from the River Murray via the Murray Bridge-Onkaparinga (MBO) Pipeline (Figure 1). Although flows in the River Murray are affected by rainfall in the basin, the upper limit of water that Adelaide has previously been able to source from the River Murray has been determined by licenses, rather than rainfall. For example, licenses have allowed for up to 90% of Adelaide’s water to be sourced from the River Murray in the past in dry years, whereas about 40% of Adelaide’s demand has been supplied by the River Murray on average [Government of South Australia, 2009]. Furthermore, and contrary to the common principle that a license does not necessarily guarantee water availability, Adelaide’s River Murray usage is almost certainly guaranteed because (1) it constitutes less than 1% of total River Murray flow; (2)

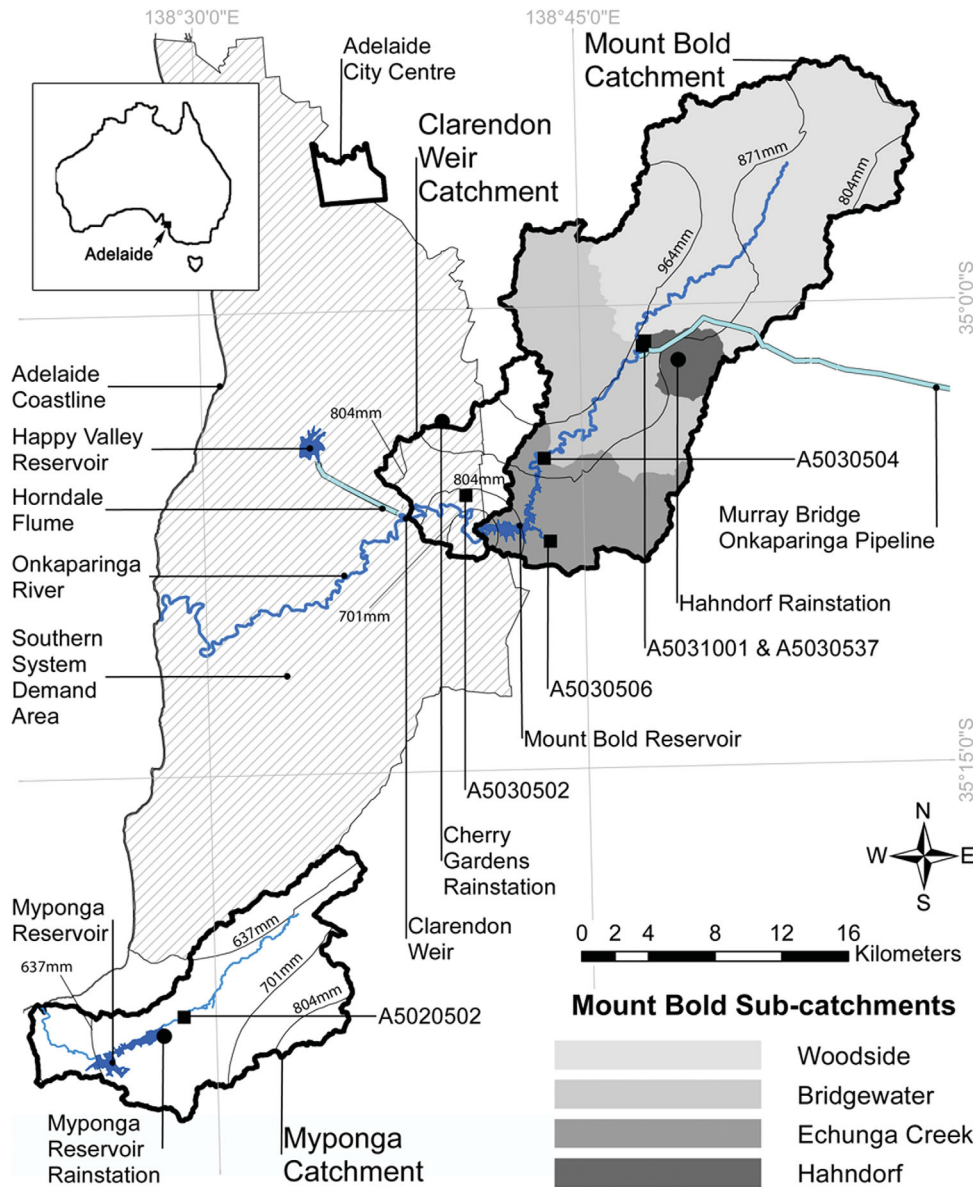


**Figure 1.** Map of Adelaide’s southern water supply system, detailing reservoirs, reservoir catchments, major rivers, pipelines, and the southern system demand area. Gauging stations, rainfall stations, Mount Bold subcatchments, and isoheytal lines that have been defined for calibrating RRO models for each catchment are also illustrated. Inset of map of Australia highlighting location of Adelaide.

critical human needs, including for Adelaide, are the highest priority in allocating River Murray water; and (3) the significant storage of the River Murray system helps to dampen out temporal variability in flow that might restrict water availability for a particular time period. The amount of River Murray water that Adelaide can use is based on a 5 year rolling license of 650 GL, with the license period beginning on 1 May each year. However, the license alone cannot supply all of Adelaide’s water demand, as the maximum River Murray supply over 5 years is about 65% of total demand. Furthermore, with projections of population growth resulting in future increases in demand, the percentage of demand potentially met by the River Murray will reduce (as the 5 year license is fixed at 650 GL). Hence,

supply from local catchments is vital in order to meet demand.

### 3. Methods

[17] Figure 2 illustrates the methodology and data used to assess water supply security at a number of discrete times in the future and the relative contributions of sources of uncertainty of climate change impacts on water supply security for Adelaide’s southern system. The first step was the development of RRO models (Figure 2), which were necessary to determine runoff from the Myponga, Mount Bold, and Clarendon Weir catchments, while the second step was to develop climate change affected rainfall and

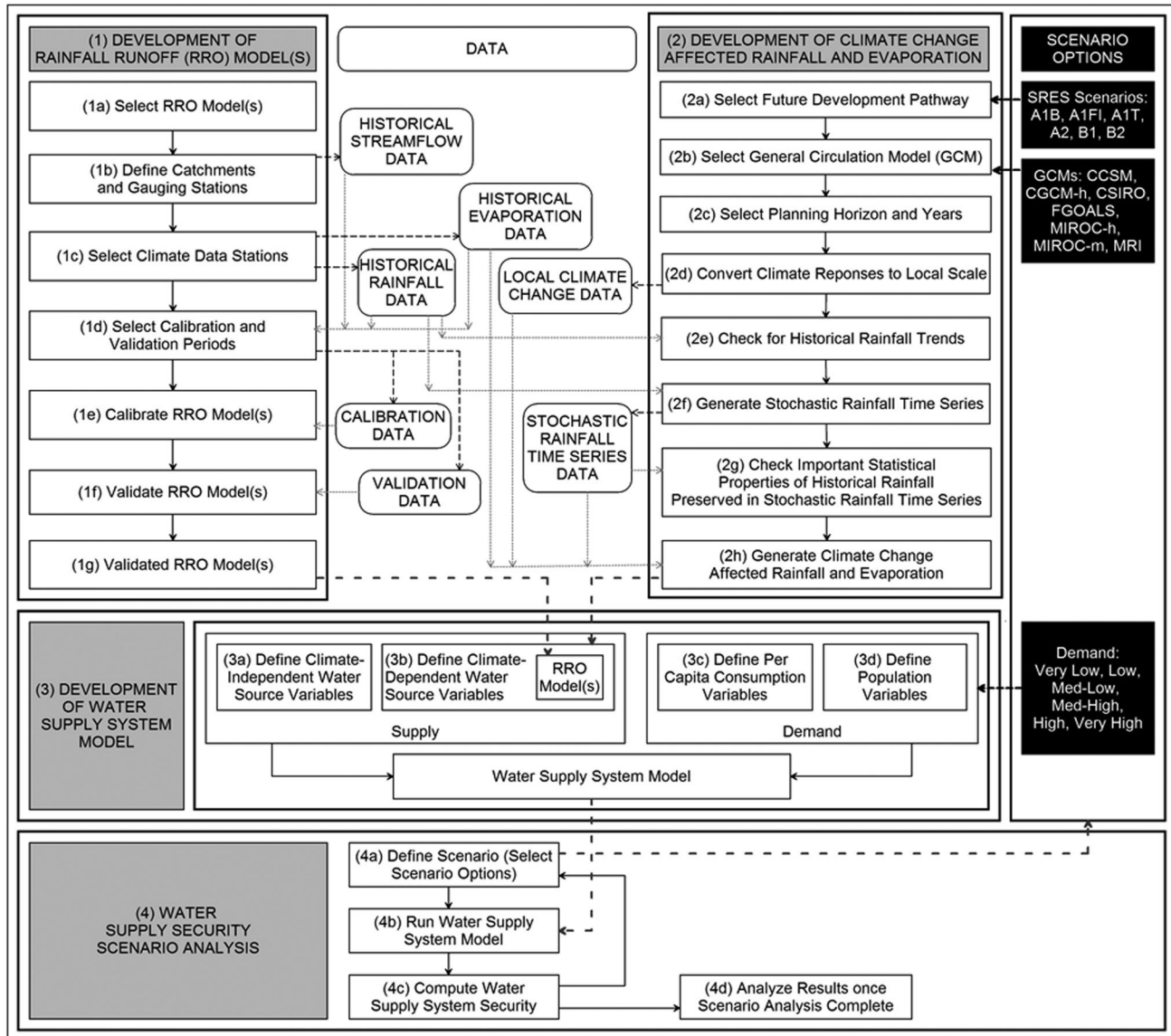


**Figure 2.** Flowchart of the methodology followed for the Adelaide southern water supply system case study.

evaporation (Figure 2). For clarity, data that were used in the case study for both the RRO models and the development of climate change affected rainfall and evaporation are highlighted in Figure 2. The validated RRO models from Step 1 and the climate change affected rainfall and evaporation from Step 2 were then applied in the development of the water supply system model for the southern Adelaide system (Figure 2). Specifically, the RRO model and the climate change affected rainfall and evaporation were used to determine supply from the climate-dependent water sources, namely the three reservoirs: Myponga, Mount Bold, and Happy Valley (Step 3, Figure 2). The supply component also incorporated the climate-independent water source of the River Murray (as explained above, see also section 3.3.1.1), while demand was a combination of per capita consumption and population (Step 3, Figure 2). Finally, in Step 4, water supply security was assessed for various uncertain water supply scenarios in a systematic

fashion, investigating uncertainties in future development pathways, GCMs, and demand (Figure 2). Steps 3 and 4 are very important because as illustrated in section 1, studies have examined the relative magnitudes of uncertainty associated with climate change impacts on runoff, but there is a need to extend this to water supply systems, for which there are additional uncertainties (e.g., demand) and additional complexities (e.g., storages).

[18] The four major steps of the flowchart are discussed in more detail in the following sections, while justification for the scenario options considered in this paper (delineated by the black boxes in Figure 2), is provided in section 3.4. While the following discussion focuses on Adelaide’s southern water supply system, the methodology presented in Figure 2 could also be readily applied to other water supply systems. However, some alterations may be required. For example, in the case study, stochastic rainfall time series were generated for a historical record and then

**Table 1.** Gauging Station Data for Each Catchment

Catchment	Catchment Area (km <sup>2</sup> )	Gauging Station Identification	Gauging Station Area (Percentage of Catchment Area) (%)	Gauging Station Data Period Available	Data Record Completeness (Percentage of Data Period Available) (%)
Myponga	124	A5020502	61	Oct. 1979–Feb. 2011	98.8
Mount Bold	388	A5030504	83	May 1973–Jan. 2011	100
		A5030506	9	Apr. 1973–Dec. 2010	97.1
		A5031001	59	Jul. 2002–Jul. 2011	99.2
		A5030537	4	Apr. 1993–Mar. 1996; Jul. 2002–Jul. 2011	98.1
Clarendon Weir	54	A5030502	49	Apr. 1969–Dec. 2010	100

perturbed for climate change, while in other cases, calibrating a weather generator on a climate change perturbed record (for example, see *Kilsby et al.* [2007]), or conditioning the parameters of a weather generator using GCM output to directly incorporate the climate change signal, may be more appropriate. In addition, the focus in this case study is on the impacts of climate change on supply; however, climate change impacts on demand could also be incorporated. For example, *Groves et al.* [2008] found outdoor water demand was projected to increase by 10% in southern California by 2040 due to the impact of climate change.

### 3.1. Development of RRO Model(s)

#### 3.1.1. Select RRO Model(s)

[19] The WC1 model was selected to determine runoff in this case study (Step 1a, Figure 2) because it has been used previously throughout the Mount Lofty Ranges [*Alcorn*, 2006; *Savadamuthu*, 2003; *Teoh*, 2002] and because it was developed based on experience with South Australian RRO calibration in the Mount Lofty Ranges and other parts of the state (see [www.watersselect.com.au](http://www.watersselect.com.au)). WC1 is a 10-parameter, conceptual RRO model that employs a three-bucket concept, in which the three storage components (or buckets) of the model are (1) interception store, (2) soil moisture store, and (3) groundwater store. Surface, interflow, and groundwater flow potentially contribute to surface runoff. Further details of the WC1 model can be found in the WaterCress user manual, available from [www.watersselect.com.au](http://www.watersselect.com.au). Both daily rainfall and monthly evaporation are required for WC1 to compute runoff.

#### 3.1.2. Define Catchments and Gauging Stations

[20] Daily flow data from gauging stations A5020502, A5030504, A5030506, and A5030502 (Figure 1) were selected for this case study (Step 1b, Figure 2) because large areas of the Myponga, Mount Bold, and Clarendon Weir catchments contribute flow at these stations and because the data sets span three to four decades and are relatively complete (Table 1). Furthermore, a catchment model of increased complexity was also defined for the Mount Bold catchment to assess the impact of model complexity on model performance. For the complex model, which contains four RRO models (one for each subcatchment), a further two suitable gauging stations for the Mount Bold catchment (A5031001 and A5030537, see Figure 1) were selected (Table 1).

[21] For each of the six gauging stations, streamflow data were sourced from the Government of South Australia's surface water archive ([www.waterconnect.sa.gov.au/SWA](http://www.waterconnect.sa.gov.au/SWA)).

Long and complete records were available for A5030502 and A5030504, long but incomplete records were available for A5030506 and A5020502, while relatively shorter and incomplete records were available for A5030537 and A5031001 (Table 1). For records that contained missing streamflow data at the very beginning or very end of the data periods, the data were excluded, while if the missing data were in the middle of the data set, they were estimated using regression analysis with nearby flow gauges. Flow records downstream of the MBO pipeline were also adjusted to take into account volumes supplied from the River Murray. Furthermore, an assessment of the rainfall and streamflow records for the Myponga catchment illustrated that from about the late 1990s, there was a marked decrease in large streamflow events but no decreasing trend in rainfall. A5020502 data were predominantly tagged as good quality, so errors in gauging seem unlikely to have caused this trend. The altered flow regime is more likely due to an increase in small farm dams and an intensification of dairying, viticulture, and olive horticulture that has occurred in the catchment over time. Consequently, calibration and validation were only carried out for Myponga catchment from January 1999 to December 2010.

#### 3.1.3. Select Climate Data Stations

[22] The Bureau of Meteorology (BoM) stations Myponga Reservoir (23738), Hahndorf (23720), and Cherry Gardens (23709) were selected as suitable climate data stations (Step 1c, Figure 2) to represent Myponga, Mount Bold, and Clarendon Weir catchments, respectively. These stations were selected because they are part of the patched point data set (PPD) [*Jeffrey et al.*, 2001], a data set comprising approximately 4600 locations around Australia and spanning from 1890 to the current day. The PPD is based on observed BoM daily meteorological records that have been enhanced by high-quality, rigorously tested data infilling (when data are missing) and deaccumulation of any records that represented rainfall over multiple days, rather than a single day [*Charles et al.*, 2008].

##### 3.1.3.1. Rainfall

[23] A number of advantages exist in using the PPD for rainfall data in this study. First, the data from each site span identical time periods with interstation correlations being upheld. Second, the data cover a long timeframe so that the existing long-term variability in rainfall experienced in Adelaide is incorporated, while third, the rainfall data are a continuous time series, which is a necessary input requirement for the modeling and analysis tools used in this study. Finally, rainfall data in the original BoM data

sets for these stations span a significant time period and are relatively complete (Table 2), ensuring that the potential errors occurring through the infilling process are minimized because the use of observed data is maximized. For example, the stations selected have greater than 90 years of rainfall records and are between 89% and 98% complete (Table 2).

[24] The climate data stations were also selected because of their location within each catchment (Figure 1), which is an important consideration in attempting to obtain an accurate representation of rainfall for a particular area because rainfall displays the largest spatial variability among meteorological variables [Srikanthan and McMahon, 2001]. In this case study, the average annual rainfall for each catchment was estimated using ArcGIS. First, all BoM stations that occurred in the PPD and that were within 15 km of the three catchments were selected. The average annual rainfalls for all stations were then spatially interpolated using the inverse distance-weighted tool and with the resulting interpolation classified into seven categories (isoheytal areas) using the Natural Breaks (Jenks) method. The average of the bounding rainfall values for each of the isoheytal areas was taken as the average rainfall for each respective area (Figure 1). These average values were then weighted by area to calculate an average annual rainfall for each of the catchments (Table 2). The resulting differences between these values and the average annual rainfall amounts for each respective climate data station were then used to create a rainfall scaling factor (Table 2), by which all daily rainfall amounts in the historical data sets were multiplied.

**3.1.3.2. Evaporation**

[25] Evaporation (which is treated as an equivalent to actual evapotranspiration in WC1) was calculated by multiplying recorded daily evaporation by the pan factor for soil (which is one of the RRO parameters to be calibrated). Recorded daily evaporation was converted from monthly Pan A evaporation inputs, which in this case study were sourced from averaging values in the PPD between 1975 and 2004 (Table 3). While the PPD contain daily evaporation values from 1889 onward, Class A evaporation pans were only installed in Australia during the 1960s [Rayner, 2005], so values in the PPD pre-1970 were interpolated from long-term averages and were thus not included. Furthermore, to develop the climate change scenarios for evaporation later in this study, evaporation data based on the 30 years from 1975 to 2004 are required (see section 3.2.3), so this 30 year period was selected.

**3.1.4. Select Calibration and Validation Periods**

[26] Approximately 60%–70% of the available data were used for calibration and 30%–40% for validation (Step 1e, Figure 2), ensuring that at least 5 years of data were used in calibration and at least 3 years were used in validation (Table 4). The calibration and validation periods for Myponga, Woodside, Hahndorf, and Bridgewater were very short, which could potentially limit the RRO models in accurately capturing the catchments’ RRO behavior, particularly if these time periods do not contain particular extreme events, such as droughts. Calibration and validation periods began in January and were multiples of 12 months, so as not to bias the RRO models’ calibrated parameters toward a particular month’s flow properties.

**Table 2.** Rainfall Station Data for Each Catchment

Catchment	Subcatchment	Climate Data Station (BoM Identification Number)	BoM Record Length	BoM Data Set Completeness (%)	Average Annual Rainfall for Climate Data Station (mm/yr)		Average Annual Rainfall for Catchment (mm/yr)		Rainfall Scaling Factor	
					Station	752	Calibration and Validation	Whole Catchment	Calibration and Validation	Whole Catchment
Myponga Mount Bold (simple) Mount Bold (complex)		Myponga Reservoir (23738)	1914–2010	89	752	736	728	0.9785	0.9677	
		Hahndorf (23720)	1884–2010	95	849	919	914	1.0828	1.0770	
	Woodside	Hahndorf (23720)	1884–2010	95	849	906	906	1.0671	1.0671	
	Hahndorf	Hahndorf (23720)	1884–2010	95	849	856	856	1.0085	1.0085	
	Bridgewater	Hahndorf (23720)	1884–2010	95	849	990	990	1.1659	1.1659	
Clarendon Weir	Echunga (& Mount Bold Reservoir)	Hahndorf (23720)	1884–2010	95	849	842	841	0.9918	0.9911	
		Cherry Gardens (23709)	1899–2010	98	929	943	859	1.0150	0.925	



**Table 3.** Average Monthly Evaporation for Climate Data Stations

Rainfall Station	Average Evaporation (mm/month)											
	Jan.	Feb.	Mar.	Apr.	May	Jun.	Jul.	Aug.	Sep.	Oct.	Nov.	Dec.
Myponga Reservoir	219	188	151	96	62	45	50	67	90	130	165	199
Hahndorf	233	201	162	102	66	47	52	72	95	139	179	213
Cherry Gardens	217	188	149	92	57	39	44	61	84	124	161	195

[27] Adelaide also suffered a severe drought from 2003 to 2009, so data from this time period alone possibly suffered from a dry rainfall bias. While it is important to understand water supply security during dry periods, it is also critical to accurately simulate runoff during wet periods as this runoff can replenish storages and potentially be used to buffer droughts. Furthermore, RRO models calibrated only on dry periods may not be able to accurately simulate the response to wet periods, so this was avoided where possible. However, it could not be helped when calibrating Woodside, Hahndorf, and Bridgewater catchments (Table 4) because of the need to use overlapping data from identical periods, a result of the Bridgewater gauging station (A5030504) being downstream of both the Woodside and Hahndorf gauging stations (A5031001 and A5030537, respectively) (Figure 1).

**3.1.5. Calibrate RRO Model(s)**

[28] A genetic algorithm (GA) was chosen over classical methods of optimization to calibrate the WC1 models (Step 1f, Figure 2), because genetic algorithms have shown to be successful in optimizing RRO models [Wang, 1991]. Upper and lower limits for each parameter for WC1 were defined to restrict the search space of the GA and ensure the physical plausibility of the parameter values. The bounds for WC1 parameters were based on limits defined in the Water-Cress user manual (see www.watersselect.com.au), which were similar to those used in the Mount Lofty Ranges, studies by Teoh [2002] and Savadamuthu [2003].

[29] Initial GA parameter trials examined populations of 100–400, generations of 100–300, and values of 0.6–0.9 for the probability of crossover, with final GA parameter selection being 200 for population, 150 for maximum number of generations, and 0.7 for probability of crossover. The probability of mutation was taken as 0.1—the inverse of the number of model parameters. In order to check whether parameter equifinality [Beven, 2006] is a potential problem, each calibration run was repeated 10 times from different

**Table 4.** Calibration and Validation Periods for Catchments and Subcatchments

Catchment or Subcatchment		Calibration Period	Validation Period
Myponga		Jan. 1999–Dec. 2006	Jan. 2007–Dec. 2010
Mount Bold (simple)		Jan. 1974–Dec. 1999	Jan. 2000–Dec. 2010
Mount Bold (complex)	Woodside	Jan. 2003–Dec. 2007	Jan. 2008–Dec. 2010
	Hahndorf	Jan. 2003–Dec. 2007	Jan. 2008–Dec. 2010
	Bridgewater	Jan. 2003–Dec. 2007	Jan. 2008–Dec. 2010
	Echunga	Jan. 1975–Dec. 1999	Jan. 2000–Dec. 2010
Clarendon Weir		Jan. 1970–Dec. 1997	Jan. 1998–Dec. 2009

starting positions in parameter space. First, there was little change in the calibration errors for the 10 trials. Similarly, the calibrated RRO parameters were reasonably stable over the 10 calibration runs, and the flows were not sensitive to these slight changes in parameters.

[30] The root-mean-square error (RMSE) of the monthly flows was selected as the performance criterion; such that RMSE was minimized in the optimization process (an RMSE equal to zero indicates a perfect fit). RMSE is biased toward minimizing error in high flows but was selected as the objective because, as mentioned in section 3.1.4, when studying water supply security, accurately simulating runoff from the large rainfall events is likely to be more important than simulating runoff from the more frequent low rainfall events, because of the ability of reservoirs to store water. If the amount of runoff from wet periods was underestimated or overestimated, the amount of water available in the storages could be quite different from reality, and would thus affect the estimated supply security during dry periods when demand exceeded runoff. Hence, high flows have the potential to have a much bigger impact on water supply security than low flows and, as such, minimizing errors in these high flows is critical. A monthly time step was chosen over a daily time step for assessing model performance because the storage of the reservoirs was likely to buffer any daily errors obtained in runoff. The average annual flows for the observed and modeled data sets and the monthly Nash-Sutcliffe (NS) were also calculated following optimization. A minimal difference between the annual observed and modeled flows and an NS value approaching one were sought. However, Jain and Sudheer [2008] point out that a high value of NS can be achieved for a model with a poor fit. Consequently, although more subjective than the use of statistical measures of goodness-of-fit, plots of simulated and observed hydrographs were also inspected following optimization. Refsgaard and Storm [1996] note that the visual inspection of plots is an efficient means of assimilating information as well as providing a good overall insight into a model’s capabilities. To compare the simple and complex Mount Bold catchment models, an additional criterion was required that could penalize model complexity as well as error. This is based on the principle that for a given level of accuracy a more parsimonious model is preferable [Bozdogan, 1987]. The application of the principle of parsimony in hydrological modeling is discussed by Wagener et al. [2004], but, in brief, complexity control is advantageous as it reduces parameter equifinality by identifying the simplest model that explains the observed data [Schoups et al., 2008]. The Akaike information criterion (AIC) [Akaike, 1973] based on monthly flows was used for this purpose.

**3.1.6. Validate RRO Model(s)**

[31] Model validation (Step 1f, Figure 2) was necessary to check that the RRO parameters optimized during calibration also performed well on independent data. A model was to be rejected as being not behavioral (i.e., not consistent with observations) [Beven, 2006] for this case study if (1) the modeled hydrographs were judged to not adequately match the observed hydrographs based on visual inspection, (2) NS was < 0.50 [Moriiasi et al., 2007], and/or (3) the RMSE was more than half the standard deviation of the observed flows [Singh et al., 2004]. Validation periods for

**Table 5.** Root-Mean-Squared Error (RMSE), Nash-Sutcliffe (NS), Ratio of RMSE to Standard Deviation (SD), and Average Observed and Modeled Flows for the Calibration and Validation Periods of the WC1 Models for the Myponga, Mount Bold (Simple), Mount Bold (Complex), and Clarendon Weir Catchments

Catchment or Subcatchment	Accuracy Criteria for Calibration					Accuracy Criteria for Validation					
	RMSE (ML/month)	NS	RMSE/SD	Average Observed Flow (GL/yr)	Average Modeled Flow (GL/yr)	RMSE (ML/month)	NS	RMSE/SD	Average Observed Flow (GL/yr)	Average Modeled Flow (GL/yr)	
Myponga	228	0.92	0.28	7.5	7.9	315	0.80	0.44	5.2	3.2	
Mount Bold (simple)	1775	0.95	0.22	51.9	51.6	1996	0.88	0.35	41.4	41.2	
Mount Bold (complex)	Woodside	798	0.90	0.31	16.9	15.8	888	0.94	0.24	20.6	17.4
	Hahndorf	122	0.74	0.51	1.9	1.6	105	0.88	0.34	2.1	1.8
	Bridgewater	1277	0.75	0.50	19.8	16.8	919	0.81	0.43	16.9	18.2
	Echunga	203	0.89	0.34	3.4	3.3	148	0.87	0.35	2.6	2.6
Clarendon Weir	134	0.94	0.25	3.9	3.9	138	0.87	0.36	3.0	3.5	

the case study were as defined in section 3.1.5, while the validation performance evaluation measures were the same as those defined above for calibration.

**3.1.7. Validated RRO Model(s)**

[32] To have confidence in using the optimized WC1 model parameters to estimate runoff for the case study, it was necessary to analyze whether the RRO models produced results within the range of accuracy identified in section 3.1.6 for the validation data. All RRO models developed for this case study had an NS > 0.50, while the RMSE values for most catchments were considered low, as they were less than 50% of their respective standard deviations, except for the calibration periods of the Hahndorf and Bridgewater subcatchments, for which they were slightly greater than 50% (Table 5). However, this was considered obsolete, because based on the NS efficiency values (Table 5) and AIC values (1515 for the complex model compared to 1480 for the simple model), it was decided the simple Mount Bold model should be used rather than the complex one. An assessment of the modeled monthly hydrographs indicated that the WC1 models recreated the observed flow hydrographs reasonably well. The WC1 model parameter values (Table 6) were similar to those obtained in previous calibration studies on nearby catchments [Alcorn, 2006; Teoh, 2002], indicating that the model parameters obtained were reasonable. Thus, the calibrated RRO models were considered valid (Step 1g, Figure 2) and could be applied to the case study with confidence.

**3.2. Development of Climate Change Affected Rainfall and Evaporation Data**

**3.2.1. Select Future Development Pathway and GCM**

[33] The first step in developing the climate change affected rainfall and evaporation data was to select the

SRES scenario to represent a future development pathway (Step 2a, Figure 2). A GCM was then selected (Step 2b, Figure 2) to translate the future emission pathway to regional climate responses. The scenario options selected for SRES scenarios and GCMs for the case study are discussed in section 3.4.1.

**3.2.2. Select Planning Horizon and Years**

[34] A planning horizon and the years for which to progressively analyze system security for the case study must be selected (Step 2c, Figure 2) to ensure that future critical points in time for water supply security will be recognized. For the case study, a 40 year period from 2010 to 2050 was selected, with 2010, 2020, 2030, 2040, and 2050 identified as regular but discrete years to analyze.

**3.2.3. Convert Climate Responses to Local Scale**

[35] The constant scaling or delta change approach was used in the case study to obtain local rainfall and evaporation responses (Step 2d, Figure 2). The constant scaling approach meant that for each month and for each climate site, the historical baseline climate was scaled by a factor representing the change projected in that month for the closest GCM grid point.

[36] Specifically, monthly factors for rainfall and areal potential evapotranspiration (equivalent to Pan A Evaporation and calculated according to the method described in Morton [1983]), were obtained from the Australian Commonwealth Scientific and Industrial Research Organization’s (CSIRO) OzClim (www.csiro.au/ozclim/). Ozclim is a tool developed for the scientific research community and policy makers that provides data on a 25 km grid over Australia. Change factors for each grid point are developed by (1) using linear regression to obtain the local change in the value of a climate variable (e.g., rainfall) per degree of global warming for a particular GCM, and (2) multiplying

**Table 6.** Parameter Values for the WC1 RRO Models for Each of the Catchments

Catchment or Subcatchment	WC1 Model Parameter									
	Median Soil Moisture (mm)	Catchment Distribution (mm)	Interception Store (mm)	Ground Water Discharge	Soil moisture discharge	Pan factor for soil	Fraction Groundwater Loss	Store Reduction Coefficient	Groundwater Recharge	Creek Loss (mm)
Myponga	160	59.4	8.1	0.0015	0.00015	0.94	0.49	0.90	0.45	0.01
Mount Bold	186	60.0	9.3	0.0015	0.00012	0.84	0.49	1.39	0.15	0.00
Clarendon Weir	195	59.5	8.0	0.0015	0.00015	0.99	0.20	0.85	0.30	0.01

this result by the degree of global warming associated with an SRES scenario. These change factors can then be applied to the baseline climatology of the climate variable (defined from 1975 to 2004), to produce future climate projections. For this case study, the change factors for rainfall and evaporation were extracted for 2020, 2030, 2040, and 2050.

[37] The delta change approach is a simple downscaling approach and has a number of limitations that include (1) the mean, maxima, and minima are the only data properties that are different between the scaled and baseline climate; (2) the spatial pattern of the present climate is assumed for the future; (3) the approach, without modification, cannot simulate changes in the occurrence of rainfall, nor changes to the size of extreme events; and (4) values for a single grid cell may contain gross biases [Wilby and Fowler, 2011]. However, the constant scaling approach was selected to downscale GCM data because (1) simple downscaling approaches can accurately simulate flow [Fowler *et al.*, 2007] and (2) the constant scaling approach can be applied easily using multiple GCMs and SRES scenarios [Mpelasoka and Chiew, 2009], which was important in this case study in order to analyze uncertainties associated with these factors.

#### 3.2.4. Check for Historical Rainfall Trends

[38] It was important that the historical rainfall time series were checked for trends before generating the stochastic rainfall time series because the stochastic rainfall generator used in this case study—stochastic climate library (SCL) (section 3.2.5), assumes that the input data (i.e., the historical rainfall) have already been checked for stationarity. Consequently, the rainfall data were run through TREND ([www.toolkit.net.au/trend](http://www.toolkit.net.au/trend)) (Step 1d, Figure 2), a tool developed by the Cooperative Research Centre (CRC) for Catchment Hydrology, which enables statistical testing for trend, change, and randomness in time series data [Chiew and Siriwardena, 2005]. As the distribution of rainfall is unknown, only the nonparametric tests were used. The Mann-Kendall and Spearman's Rho tests were used to test for a trend; the distribution-free Cumulative Sum (CUSUM) was used to test for a step jump in the mean; while the rank-sum test was used to check for a difference in median between two sections of the data set. In this case study, rainfall from May 1974 to April 2004 was elected as the baseline data from which to derive future climate change scenarios because 1975 to 2004 is the OzClim baseline (see section 3.2.3), and the River Murray license year runs from 1 May to 30 April (see section 2). Consequently, rainfall data from the three sites spanning this time period were analyzed in TREND. For each of the three rainfall stations, none of the aforementioned tests returned a significant result (indicating that there were no trends or step jumps in the nominated time series), apart from the Mann-Kendall test for Hahndorf. However, the significance level of this test suggested that there was little evidence of a trend, and given the Spearman's Rho test (which also tests for a trend) did not return a significant result, it was presumed that if such a trend in the Hahndorf data set existed, it was insignificant for the purpose of this study.

#### 3.2.5. Generate Stochastic Rainfall Time Series

[39] Generating stochastic rainfall time series for the case study (Step 2e, Figure 2) was important because urban

water supply planning should include the stochasticity in precipitation [O'Hara and Georgakakos, 2008] and because Adelaide has such high, natural temporal rainfall variability (see section 2). Use of stochastic rainfall data ensured that (1) the results produced were not simply a reflection of the historical rainfall time series, and (2) water supply system security could be reported as a distribution to reflect the inherent variability in historical rainfall, rather than a single deterministic value. A probability-based approach is particularly useful from a water management perspective because it establishes ranges and confidence levels to help understand future levels of risk to the system. It is important to note that while this distribution will reflect historical rainfall variability, it does not necessarily reflect future rainfall variability. To correctly achieve projections of future rainfall variability would require applying a perturbed physics ensemble or weather generator to generate rainfall sequences based on climate characteristics. For example, a weather generator could be calibrated on a climate change perturbed record or its parameters could be conditioned on large-scale atmospheric predictors, weather states, or rainfall properties to directly incorporate climate change [Wilby and Fowler, 2011]. These methods are beyond the scope of this paper.

[40] The stochastic rainfall time series were constructed using the multisite daily rainfall model of the SCL ([www.toolkit.net.au/scl](http://www.toolkit.net.au/scl)), developed by the CRC for Catchment Hydrology [Srikanthan, 2005]. It is a multisite two-part daily model, nested in a monthly and annual model. The first part consists of rainfall occurrence, which is determined using a first-order two-state Markov chain, while the second part relates to rainfall amounts, derived using a gamma distribution [Srikanthan, 2005]. This daily model is then nested in a monthly and annual model in order to preserve the monthly and annual characteristics. The monthly and annual models are driven by the noise term derived from the generated daily rainfall data. The mathematical development of the monthly and annual models is provided by Srikanthan [2005] and Srikanthan and Pegram [2009]. Because of the great spatial variability of rainfall (see section 3.1.3.1), a multisite model was necessary to account for the spatial dependence between rainfall stations, while the SCL was selected because it preserves the important characteristics of rainfall at daily, monthly, and annual time scales [Srikanthan, 2005].

#### 3.2.6. Check Important Statistical Properties of Historical Rainfall Preserved in Stochastic Rainfall Time Series

[41] Statistical analyses of the developed stochastic time series were necessary to ensure that the important statistical properties of the historical data were preserved in the stochastic time series (Step 2f, Figure 2). Srikanthan *et al.* [2004] provide suggested tolerances for each statistical parameter but also suggest that users make their own assessment of the quality of the data produced by SCL because certain statistics may be more important than others depending on the application. First of all, because these stochastic time series represent natural rainfall variability, measures of variability (e.g., standard deviation) must be assessed and because of the high interannual and interdecadal variability experienced by Adelaide (see section 2), preservation of interannual and interdecadal variability was

**Table 7.** Important Annual Statistical Properties of the Historical and Generated Rainfall Time Series

Parameter	Unit	Climate Data Station						
		Hahndorf		Cherry Gardens		Myponga		
		Historical	Generated	Historical	Generated	Historical	Generated	
Mean	mm/yr	794	794	905	906	756	756	
Standard deviation	mm/yr	158	159	145	146	163	163	
Maximum	mm/yr	1248	1139	1335	1220	1111	1113	
Minimum	mm/yr	479	487	665	619	467	444	
Low rainfall sums	2-yr	mm/2yrs	1188	1204	1441	1452	1107	1087
	3-yr	mm/3yrs	1931	1938	2261	2301	1852	1771
	5-yr	mm/5yrs	3474	3452	4140	4044	3316	3197
	7-yr	mm/7yrs	4975	5003	5864	5821	4626	4663
	10-yr	mm/10yrs	7368	7375	8665	8530	6813	6920

also necessary. For this case study, the 2-, 3-, 5-, 7-, and 10-year low rainfall sums were particularly important, because the accumulation of a number of years with below-average rainfall creates water supply security concerns, rather than a single year. This is because Adelaide currently has the ability to buffer an extremely low rainfall year through reservoir storage and pumping water from the River Murray with a 5 year rolling license, whereas an accumulated dry spell of a number of years may result in reservoirs running dry and the River Murray license being fully allocated. The annual mean rainfall was also considered an important measure, so as not to overpredict or underpredict runoff. Furthermore, the coincidence of below-average rainfall years across the three rainfall sites could also impact total water supply from the reservoirs, so matching the observed annual cross correlation between rainfall sites was also important.

[42] For the case study, 1000 stochastic rainfall time series of 30 years were developed. Differences between the annual standard deviation of the historical and generated series for all sites (Table 7) were no greater than 1 mm/yr, which is well within the tolerance of 5 mm/yr suggested by *Srikanthan et al.* [2004]. Similarly, differences in the maximum and minimum annual rainfall values for all three sites (Table 7) fell within the 10% tolerance suggested by *Srikanthan et al.* [2004]. The average difference in multiyear rainfall sums was 1.5%, with all multiyear rainfall sums (Table 7) well within the 10% tolerance suggested by *Srikanthan et al.* [2004]. The mean annual rainfall amounts in the generated data for the three sites (Table 7) were within 0.02% of the historical means, while the average difference in mean monthly rainfall amounts for the three sites was 2.0%, with only the February rainfall for Hahndorf and March rainfall for Cherry Gardens, not being within the 7.5% tolerance suggested by *Srikanthan et al.* [2004]. Finally, the differences in annual cross-correlation values between the three rainfall sites ranged from 0.01 to 0.04, well within the tolerance of 0.2 suggested by *Srikanthan et al.* [2004]. Consequently, based on the similarity in statistical properties that were considered important to this case study, the generated stochastic data were considered to preserve the important characteristics of the historical rainfall and were thus appropriate for further use in this study. However, it is recognized that the time period elected to base the stochastic rainfall time series on (30 years from 1974 to 2004), is relatively short and may therefore not

represent the true natural rainfall variability of the system. While longer time periods were considered to increase the representation of natural rainfall variability, the average monthly mean rainfalls of the longer data sets were considerably different to those for OzClim's 30 year baseline (see section 3.2.3) and so could not be used in this case study.

### 3.2.7. Generate Climate Change Affected Rainfall and Evaporation

[43] Climate change affected rainfall and evaporation were subsequently developed by applying the percentage changes obtained from OzClim to the stochastic rainfall time series and the historical evaporation data, respectively (Step 2g, Figure 2). A caveat of this methodology is that the stochastic rainfall time series and historical evaporation data are not mutually consistent, which may affect daily runoff because it is a response to both of these variables acting together. However, uncorrelated daily rainfall and evaporation are not expected to influence water supply system security because the storage of the reservoirs is likely to buffer any daily errors obtained in runoff. Furthermore, evaporation is less variable compared with rainfall; for example, for the baseline period of 1974–2005 for Kent Town, the average standard deviation of evaporation per month was approximately half of that for rainfall.

### 3.3. Development of Water Supply System Model

[44] The water supply system model consisted of both supply and demand components, with supply requiring the definition of climate-independent (Step 3a, Figure 2) and climate-dependent (Step 3b, Figure 2) water sources and demand requiring per capita consumption (Step 3c, Figure 2) and population (Step 3d, Figure 2) variables to be defined. Climate change affected rainfall and evaporation data from Step 2 were used to determine supply from the reservoirs (climate-dependent sources), while the validated RRO models of Step 1 were used to calculate runoff from the catchments that flowed into the reservoirs (Figure 2).

#### 3.3.1. Water Supply System Model

[45] The continuous time series, water resources model WaterCress (available from [www.watersselect.com.au](http://www.watersselect.com.au)), was chosen for this case study because it can not only balance supply and demand and uphold system constraints but also (1) readily incorporate multiple rainfall time series (see section 3.2.5), (2) model multiple catchment-reservoir relationships, (3) incorporate an external supply to represent the River Murray, and (4) output data to easily compute

**Table 8.** Monthly Mount Bold Reservoir Levels (as a Percentage of Full Capacity) That Trigger Use of River Murray Supply

Jan.	Feb.	Mar.	Apr.	May	Jun.	Jul.	Aug.	Sep.	Oct.	Nov.	Dec.
90%	90%	90%	90%	2%	2%	2%	2%	2%	2%	80%	90%

water security. Furthermore, the model is freely available and has the advantage of being developed and supported within South Australia.

**3.3.1.1. Supply**

[46] As mentioned in the introduction to section 3, both climate-dependent and climate-independent supply sources were defined for Adelaide’s southern system. For Adelaide, the availability of River Murray supply is dictated by licenses, rather than by climate, and as Adelaide only takes about 1% of River Murray flow, the amount prescribed is virtually guaranteed, irrespective of climatic conditions (see section 2). Consequently, the River Murray supply was considered a climate-independent source for this case study, with its 5 year rolling Adelaide license of 650 GL converted to an annual license and then reduced by half to represent the southern system demand. Consequently, supply from the River Murray was capped at 65 GL/yr, with a year defined as being from 1 May to 30 April. Simplifying the 5 year rolling license to an annual license was necessary due to limitations of the water supply system model. This simplification is therefore considered a conservative approach because it has the potential to underestimate water supply security. The daily pumping capacity for the MBO pipeline of 447 ML/day (see www.sawater.com.au) was also defined as a constraint in the model. Furthermore, water was only pumped from the River Murray when the volume of water in Mount Bold Reservoir dropped below the levels defined in Table 8 (provided that the annual cap of 65 GL had not already been reached). These levels were calibrated in WaterCress using a trial-and-error approach in order to provide a balance between minimizing the loss of water through spillage (due to the reservoir exceeding full capacity) and maximizing water supply security.

[47] To simplify the reservoir modeling and because of the relationship between Clarendon Weir and Happy Valley Reservoir (see section 2), these two storages were treated as a single reservoir and are hereafter referred to as Happy Valley Reservoir. Water was supplied from Myponga reservoir and Happy Valley reservoir (which included water from Clarendon Weir catchment, Mount Bold catchment, and the River Murray) in equal priority and equal proportions, provided that water was available in each of the reservoirs. For Myponga, Mount Bold, and Happy Valley

**Table 9.** Properties of Mount Bold, Happy Valley, and Myponga Reservoirs

Reservoir	Minimum Volume (GL)	Maximum Volume (GL)	Volume-Area Relationship Parameters	
			a	b
Myponga	4.6	26.8	0.2729	0.68
Mount Bold	0.4	46.2	0.2073	0.68
Happy Valley	4.5	11.9	0.3066	0.68

Reservoirs, evaporation and rainfall data were obtained from the same climate data stations as used for their respective catchments (see section 3.1.3). Minimum volumes were taken as the physical minimum operating levels as per *Crawley* [1995], and maximum volumes were as specified by SA Water (see section 2) (Table 9). The first of the two mathematical expressions provided in WaterCress were used to describe the reservoir volume-area relationships (which enabled evaporation losses from the reservoir surface to be computed):

$$SA = aV^b, \tag{1}$$

where SA is the surface area of the reservoir (hectare), *V* is the volume of the reservoir (ML), and *a* and *b* are parameters. For each reservoir, the resulting value for the volume-area relationship parameter *a* (Table 9) was determined by assuming the reservoir was at full capacity and holding the other volume-area relationship parameter *b* at 0.68 (the default value in WaterCress). This equation and parameter selection appeared reasonable, as when the modeled surface areas for Mount Bold reservoir were compared to measured values provided by *Crawley* [1995], there was generally less than 2% difference over a broad range of volumes.

**3.3.1.2. Demand**

[48] In 2008, Adelaide’s total mains water consumption, with severe water restrictions in place, was approximately 166 GL (effectively 83 GL for the southern system), with water restrictions estimated to have saved 50 GL for the whole of Adelaide [*Government of South Australia*, 2009]. However, because water restrictions have now been lifted in Adelaide, demand for the southern system was modeled at the higher rate of 108 GL for 2010. This demand was assumed to be a function of individual per capita consumption and population, and both of these variables were adjusted on an annual basis over the 40 year planning horizon to constitute the demand scenario options (see section 3.4.1).

[49] Initial individual per capita consumption for the case study was based on the breakdown of demand between sectors in Adelaide for 2008, such that 63% was accounted for by the residential sector (with 40% of this demand attributed to outdoor use and 60% attributed to in-house use), while the remaining 37% was split between primary production, industrial, commercial and public purposes, and other [*Government of South Australia*, 2009]. Thus, total annual demands for the southern system in 2010 were assumed to be 40.8 GL for residential indoor use, 27.2 GL for residential outdoor demand, and 40.0 GL for nonresidential demand. Due to Adelaide’s high natural intra-annual rainfall variability, outdoor demand in Adelaide also varies with time of year. Consequently, outdoor residential demand was varied using the percentages of exhouse usage estimated by *Barton* [2005] for Adelaide (Table 10).

[50] Adelaide’s population in 2010 was about 1.2 million people, so assuming the southern system demand is approximately half of Adelaide’s demand (see section 2), the initial population for the southern system was assumed to be approximately 600,000 people. Australia’s average household size in 2001 was 2.6 people, while in 2026, this is projected to decrease to between 2.2 and 2.3 people, a

**Table 10.** Monthly Outdoor Water Use as a Percentage of Total Annual Outdoor Water Use [Barton, 2005]

Jan.	Feb.	Mar.	Apr.	May	Jun.	Jul.	Aug.	Sep.	Oct.	Nov.	Dec.
22.9%	18.8%	14.2%	6.4%	3.0%	0.0%	0.1%	0.7%	1.4%	4.9%	10.7%	17.0%

reflection of the increase in single-person households [Australian Bureau of Statistics, 2008]. For simplicity in the modeling, average household size was held at a constant 2.3 people throughout the planning period.

### 3.4. Water Supply Security Scenario Analysis

#### 3.4.1. Define Scenario (Select Scenario Options)

[51] For the water supply security scenario analysis, scenario options were selected (Step 4a, Figure 2) in accordance with the objectives of the paper. Sixteen scenario options were defined to (1) assess the relative magnitude of the impacts of major sources of uncertainty and (2) identify critical points in the future for water supply security for Adelaide's southern water supply system. Average, best, and worst cases were defined to project a likely scenario and establish likely bounds of water supply security for Adelaide's southern water supply system.

##### 3.4.1.1. Scenarios to Assess the Relative Magnitudes of Major Sources of Uncertainty and Identify Critical Points in the Future for Water Supply Security for Adelaide's Southern Water Supply System

[52] Different SRES scenarios, GCMs, and demands were considered as scenario options in the case study (Figure 2). The six SRES scenarios of A1B, A1FI, A1T, A2, B1, and B2 were selected (Figure 2) to cover the full range of potential future development pathways defined by the IPCC. The A1B scenario explores the situation of rapid economic growth and introduction of new and efficient technologies, a peak in global population at about 2050 and a balance across all energy sources, while A1FI and A1T are based on the same assumptions except in terms of technological advancement; A1FI assumes intense fossil fuel use while A1T assumes a non fossil fuel-directed future [Intergovernmental Panel on Climate Change, 2007]. A2 assumes a future with high population growth, slow economic growth, and gradual technological development; B1 reflects the same population outcomes as the A1 family but with quicker changes in economic structures to enable a service and information economy; while B2 represents intermediate population and economic growth with a focus on local sustainable solutions [Intergovernmental Panel on Climate Change, 2007].

[53] In selecting GCMs for this case study, CSIRO's Climate Futures Framework (CFF) [Clarke et al., 2011] was applied, in which plausible climates simulated by GCMs for different SRES scenarios are classified into a small set of representative climate futures (RCFs) defined by, and represented by, a matrix of two climate variables [Whetton et al., 2012]. Consequently, a smaller subset of models can be selected that covers the identified RCFs to reduce computational effort but still address the uncertainty in GCM projections. Skill-based GCM assessments are another method used to define smaller subsets of GCMs, but these suffer from (1) the assumption that a good estimation of past climate correlates with a good estimation of future

climate, and (2) the lack of a robust method [Whetton et al., 2012], and community-agreed metric [Perkins and Pitman, 2009], to use when attempting to identify "best performing" models.

[54] Before constructing the RCFs and in consultation with a CSIRO climate scientist, five GCMs were removed from the 24 available CGMs in the CFF (23 CMIP GCMs and CSIRO's Mk3.5 model) because they did not simulate the El Niño-Southern Oscillation (ENSO) phenomenon (L. Webb, personal communication), which was critical because (1) Adelaide's climate is influenced by ENSO interannual variability and (2) natural climate variability is important for this case study. The five GCMs excluded based on their poor simulation of ENSO were INM-CM3.0, PCM, GISS-EH [Irving et al., 2011], GISS-AOM, and GISS-ER [Irving et al., 2011; van Oldenborgh et al., 2005].

[55] The two indices used to categorize the models into RCFs for this case study were annual change in rainfall and annual change in temperature. Temperature was used as a surrogate for evaporation because (1) there exists a 90% correlation between temperature and potential evaporation for Australia [Whetton et al., 2012] and (2) evaporation data were only available for eight of the GCMs, while temperature data were available for all 19 models.

[56] Using these models and indices, six RCFs were defined for the Adelaide and Mount Lofty Ranges region for the A1B scenario in 2050, ranging from "warmer with little precipitation change" to "hotter and much drier." However, only five RCFs from this matrix were represented by the seven GCMs in OzClim that (1) were not eliminated based on poor ENSO simulation and (2) had both rainfall and evaporation data available. Maintaining physically consistent combinations of rainfall and evaporation data was necessary in order to maximize the robustness of the impact assessment [Clarke et al., 2011]. The GCMs in OzClim were CCSM3 (hereinafter CCSM), CGCM3.1(T63) (hereinafter CGCM-h), CSIRO-MK3.5 (hereinafter CSIRO), FGOALS-g1.0 (hereinafter FGOALS), MIROC3.2(hires) (hereinafter MIROC-h), MIROC3.2(medres) (hereinafter MIROC-m), and MRI-CGCM2.3.2 (hereinafter MRI). These seven GCMs did not represent the "warmer and much drier" RCF but they still represented the most and least severe RCF. Furthermore, while three of these models fell within the same RCF, they were all included in the case study, because the RCF matrix only examined annual changes to the variables, while monthly changes are analyzed in the case study, which are potentially dissimilar between models.

[57] Six demand options were investigated to cover a broad range of potential future demand scenarios (Figure 2), constituted from two per capita consumption projections and three population projections (Table 11). The first individual per capita consumption case (labeled Reduction, Table 11) included a reduction in per capita consumption due to the effects of permanent water conservation measures, savings due to government incentives and increasing water price, and increases in the use of water-efficient technologies. By 2050, total water savings due to demand management strategies for Adelaide are expected to be 48 L/capita/day (Lcd) for households and 21 Lcd for other demands [Government of South Australia, 2009]. *Water for Good*

**Table 11.** Demand Scenario Options

Demand Scenario	Per Capita Consumption	Population
Very low	Reduction	Small
Low	Constant	Small
Medium low	Reduction	Medium
Medium high	Constant	Medium
High	Reduction	Large
Very high	Constant	Large

does not differentiate the 48 Lcd savings between in-house and ex-house use; however, the preceding water security plan for Adelaide, *Waterproofing Adelaide: A Thirst for Change 2005–2025* [Government of South Australia, 2005], provides an estimate of the breakdown to 2025. For example, in-house measures such as low-flow showerheads, water-efficient washing machines, and dual-flush toilets are projected to account for about 37% of household savings by 2025, while permanent water conservation measures, urban consolidation, more efficient practices, and low water use vegetation are expected to contribute the remaining 63% of household savings [Government of South Australia, 2005]. Consequently, annual linear (i.e., noncompounded) percentage decreases were applied to per capita consumption over the 40 year planning horizon to account for demand management savings; residential indoor use was reduced by 0.237% per annum, residential outdoor demand was reduced by 0.606% per annum, while nonresidential demand was reduced by 0.281% per annum. The second case (labeled “constant,” Table 11) reflected the possibility that no savings in individual per capita consumption would be made over the planning horizon, such that individual per capita consumptions remained constant over the planning horizon at 187 Lcd for residential indoor demand, 124 Lcd for residential outdoor demand, and 183 Lcd for nonresidential demand. The impacts of climate change on demand have not been investigated in this study because future projections are not available for Adelaide. Furthermore, while demand is affected by weather and climate factors

[House-Peters and Chang, 2011], it is also a response to the complex interaction of multiple variables, including economic and social factors (e.g., water pricing); consequently, projecting the impacts of climate change on demand is not as straightforward as simply correlating demand to climate variables. However, the constant variation defined above can be considered a very conservative approach to demand projection and thus does not only reflect the possibility of “no savings” but could represent the possibility of making some savings (which is highly likely) in combination with increasing demand due to climate change.

[58] Taking into account fertility, mortality, net interstate migration, and net overseas migration rates, the Australian Bureau of Statistics’ (ABS) median population projection (from 72 population projections) for Adelaide in 2050 is approximately 1.56 million people [Australian Bureau of Statistics, 2008]. Therefore, the first population case (labeled “medium,” Table 11) applied a linear (i.e., noncompounded) percentage increase of 0.736% per year to the southern system population. Two additional population options (labeled “small” and “large,” Table 11) were also defined to investigate futures with small and large populations. Consequently, the 5th and 95th percentile values of the 72 population projections made by the ABS for Adelaide were used, corresponding to annual linear percentage changes of  $-0.680%$  (small) and  $1.579%$  (large), respectively. The resulting demand scenarios formulated from combinations of the two per capita consumption cases and the three options for population are labeled very low, low, medium-low, medium-high, high, and very high (Table 11).

[59] A “base case,” from which to compare the scenario options, was defined as a combination of the A1B SRES scenario, the FGOALS GCM, and the medium-low demand scenario (base case, Table 12). As no likelihoods have been assigned to the SRES scenarios [Intergovernmental Panel on Climate Change, 2007], the A1B SRES scenario was selected for the base case as it represents a median GHG emissions future compared to the other SRES scenarios.

**Table 12.** Scenario Options Defined for the Case Study of Adelaide’s Southern Water Supply System

Scenario Options		Scenario ID																Best Case	Worst Case		
		Base Case	1	2	3	4	5	6	7	8	9	10	11	12	13	14	15			16	
SRES Scenario	A1B	x						x	x	x	x	x	x	x	x	x	x	x			
	A1FI		x																		x
	A1T			x																	
	A2				x																
	B1					x															x
	B2						x														
GCM	FGOALS	x	x	x	x	x							x	x	x	x	x				
	CCSM						x														x
	CGCM-h							x													
	CSIRO								x												x
	MIROC-h									x											
	MIROC-m										x										
Demand	MRI										x										
	Medium High	x	x	x	x	x	x	x	x	x	x	x									x
	Very Low												x								
	Low														x						
	Medium Low															x					
	High																x				
Very High																	x				x

FGOALS was selected for the base case because the percentage of models supporting an RCF may be considered as providing an indication of relative likelihood [Whetton *et al.*, 2012], and out of the seven selected GCMs, it was the only GCM that represented the RCF supporting the highest percentage of GCMs. Furthermore, FGOALS represented a “warmer and drier” future climate, which is a middle of the range projection. The medium-low demand scenario was selected because the per capita consumption rate with water savings is projected for Adelaide, while a medium population is more likely to occur than either the small or large population projections. The remaining 16 scenarios used to test the magnitude of uncertainty sources are summarized in Table 12, with scenarios 1–5 used to compare across the SRES scenarios, scenarios 6–11 used to compare GCM selection, while scenarios 12–16 are used to compare different demand projections. In each of these scenarios, there is only one change made to the base case, so that uncertainty due to a particular source can be isolated.

[60] While an almost infinite number of possible scenario combinations could have been explored, it was appropriate to limit the scenarios to those listed in Table 12 as these scenarios ensured that the major sources of uncertainty were examined while keeping computational effort reasonable, and thus the first objective of the paper could be met. The impacts on water supply security of other sources of uncertainty, such as the downscaling model, GCM initial conditions, RRO model, and RRO model parameters were not examined in the case study for reasons discussed below.

[61] A caveat of this study is that rainfall and evaporation data sets derived from different downscaling methods are not available and thus the impact of the downscaling model on supply reliability could not be tested as a source of uncertainty. However, in previous studies of the impact of climate change on runoff, downscaling models were shown to contribute less uncertainty than GCMs [Boé *et al.*, 2009; Chen *et al.*, 2011a, 2011b; Mpelasoka and Chiew, 2009; Wilby and Harris, 2006], less uncertainty than SRES scenarios [Chen *et al.*, 2011a, 2011b], and less uncertainty than GCM initial conditions [Chen *et al.*, 2011b] (see section 1). Direct comparisons of downscaling approaches are also difficult to achieve because they use different spatial domains, predictor variables, predictands, and assessment criteria [Fowler *et al.*, 2007]. GCM initial conditions were not examined in the case study because (1) the authors did not run the GCMs and (2) the data sourced from OzClim did not include multiple ensemble runs.

[62] Different RRO models and their parameters were also not tested in the case study because Chiew *et al.* [2009a] illustrated that RRO models exhibited less uncertainty in determining the impacts of climate change on runoff than GCMs; Chen *et al.* [2011b] illustrated that in estimating runoff under climate change impacts, hydrological models and hydrological model parameters contributed less uncertainty than GCMs, GCM initial conditions, and GHG emissions scenarios; while Wilby and Harris [2006] showed hydrological models and their parameters contributed less uncertainty in estimating runoff under climate change impacts than GCMs (see section 1). However, Wilby and Harris [2006] did show that hydrological models

and their parameters contributed more uncertainty to estimating runoff under climate change impacts than SRES scenarios, so this study is limited in that it only assesses one RRO model and one set of RRO model parameters.

[63] It should be noted that the relatively insensitive responses of runoff to the downscaling model and the choice of RRO model and parameters, compared to other sources of uncertainty, cannot necessarily be generalized to other cases. However, a water supply manager with limited resources for impact assessments must make some assumptions as to the importance of uncertainty sources based on previous case studies to ensure effort is directed toward the greatest expected sources of uncertainty.

#### 3.4.1.2. Scenarios to Project Ranges of Water Supply Security for Adelaide’s Southern Water Supply System

[64] To project the likely range of the impact of climate change on water supply security for Adelaide’s southern water supply system (and thus address the third objective of this paper), best and worst cases were defined, with scenario options only selected from those detailed in section 3.4.1.1. For the best case, the very low demand scenario was selected, while for the worst case, the very high demand scenario was selected (Table 12). However, it was not so clear which SRES scenario and GCM would be associated with the lowest and highest water supply securities. Consequently, the SRES scenarios and GCMs for the best and worst cases were selected after the base case and scenarios 1–11 (Table 12) were run and analyzed. Following this analysis (section 4.1), B1 was found to return the highest water supply security and thus was selected for the best case (Table 12), while choosing A1FI resulted in the lowest water supply security at the end of the planning horizon, so it was selected for the worst case (Table 12). Similarly for the GCMs, CGCM-h was selected for the best case because it returned the highest reliability in 2050, while CSIRO was selected for the worst case as it corresponded to the smallest reliability for all years (Table 12). The results for these best and worst cases were discussed in reference to those obtained for an “average” case, which for this case study was defined as scenario 6 (Table 12). The average case was different to the base case, because the base case was composed of a combination of the most likely projections, or when there was no understanding of their likelihood of occurrence, median projections were used (e.g., for population growth). Consequently, while the A1B scenario and medium-low demand scenarios were appropriate to use for both the base case and average case (see Figures 3, 6, and 7), CCSM provided reliabilities that were closer to representing the average for the GCM scenarios than FGOALS, which was used for the base case (see Figures 4 and 5).

#### 3.4.2. Run Water Supply System Model and Compute Water Supply System Security

[65] The scenarios listed in Table 12 were run through the WaterCress model (Step 4b, Figure 2) for each of the 1000 stochastic rainfall time series for 2020, 2030, 2040, and 2050. Water supply system security, represented by reliability calculated on a daily time step for the case study, was then determined for each scenario (Step 4c, Figure 2). Reliability was selected to represent water supply system security for the case study because it provides information as to the proportion of time spent in failure, an important factor in understanding water supply security.



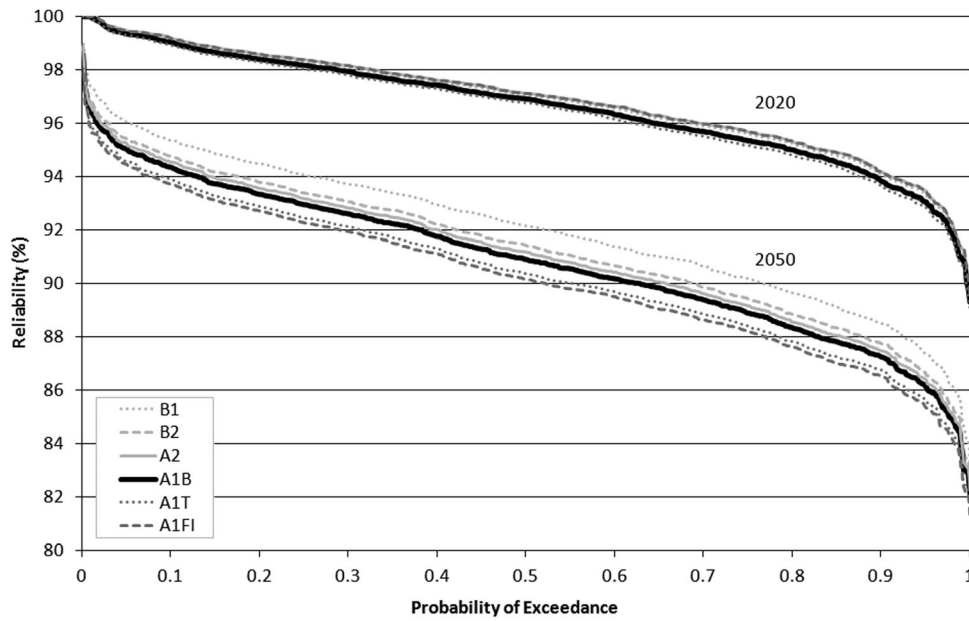


**Figure 3.** The cdf of reliability (based on 1000 stochastic rainfall time series) of Adelaide’s southern water supply system for different SRES scenarios for 2020 and 2050.

[66] Reliability for each of the future years is defined as

$$R_{yi} = \frac{T_{syi}}{T_{tyi}}, \quad (2)$$

where  $R_{yi}$  is the reliability for stochastic time series  $i$  ( $i = 1 - 1000$ ) for year  $y$  ( $y = 2010, 2020, 2030, 2040, \text{ or } 2050$ ),  $T_{syi}$  is the total number of days that available supply exceeds demand for stochastic time series  $i$  and year  $y$ , and  $T_{tyi}$  is the total number of days for stochastic time series  $i$  and year  $y$ . For each year and for each of the 1000 stochastic rainfall time series (developed in Step 2e of Figure 2),

the model was run and reliability was computed (Equation (2)), such that for each scenario, 1000 different reliabilities were calculated. Consequently, reliability could be presented as a probability (based on the 1000 stochastic rainfall time series), rather than a deterministic value. This meant that uncertainties in natural rainfall variability, expressed by the probabilities of reliability for each scenario, could be analyzed and compared to the uncertainties in selecting SRES scenarios, GCMs, and demand.

[67] From a planning perspective, it is also important to understand how reliability changes through time so that

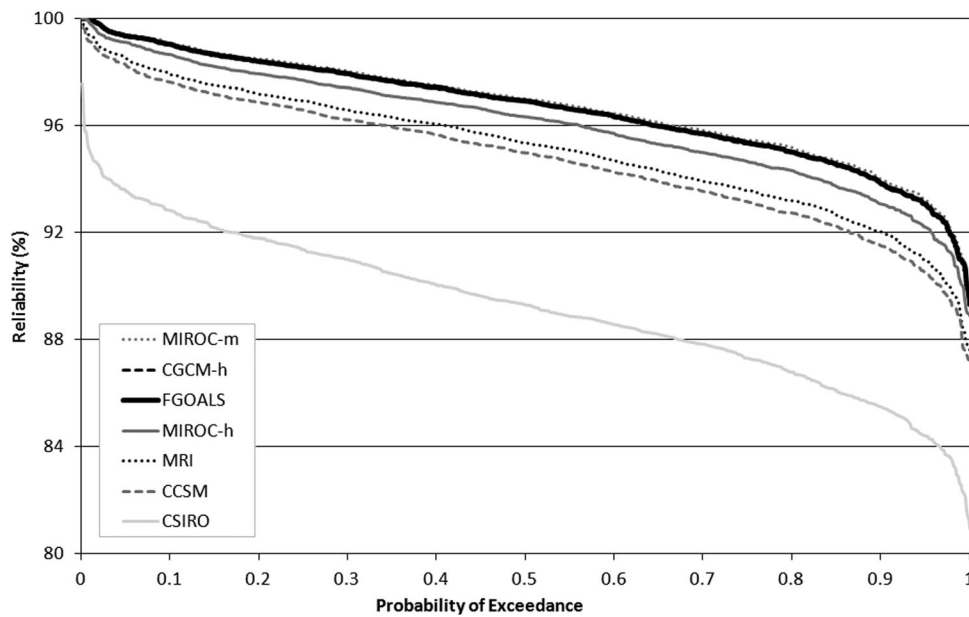


**Figure 4.** The cdf of reliability (based on 1000 stochastic rainfall time series) of Adelaide’s southern water supply system for different GCMs for 2020.

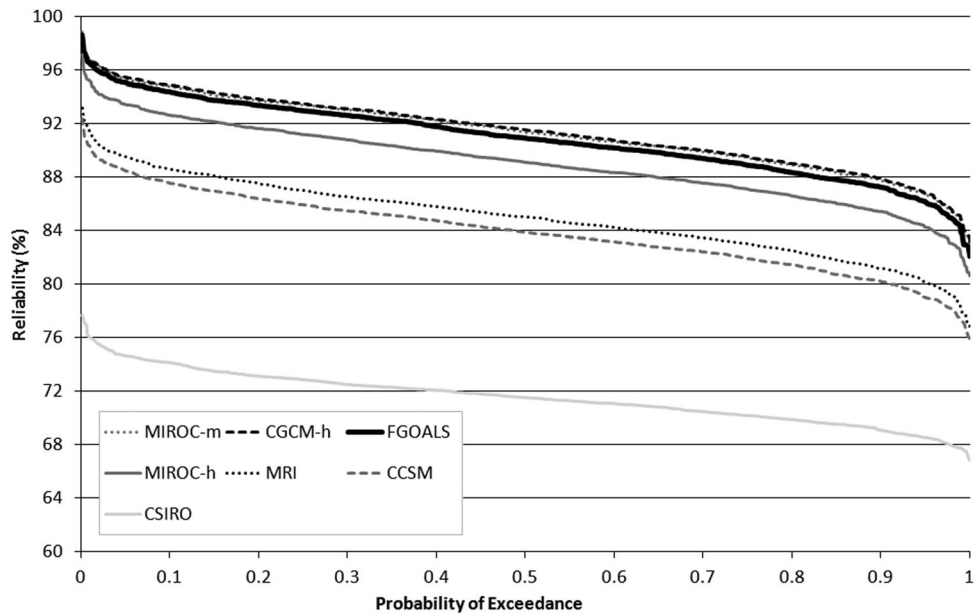


**Figure 5.** The cdf of reliability (based on 1000 stochastic rainfall time series) of Adelaide’s southern water supply system for different GCMs for 2050.

additional supply or demand management schemes can be sequenced to come on line when they are required to raise reliability to an acceptable level (see section 1). Consequently, changes in reliability between years over the planning horizon were also analyzed by linear interpolation.

**4. Results and Discussion**

[68] The analysis of reliability in section 4.1 addresses the first objective of this paper, which is to understand the relative magnitudes of major sources of uncertainty when

analyzing the impacts of climate change on water supply security. It is important to note that the cumulative distribution functions (cdf) presented herein purely reflect the stochastic nature of the natural rainfall variability, rather than any other systematic uncertainty. Changes in reliability over the planning horizon are then analyzed in section 4.2 in order to illustrate future critical points in time for water supply security and thereby address the second objective of the paper. Finally, section 4.3 examines the best and worst cases to understand water supply security ranges projected for Adelaide’s southern system, thus satisfying the third

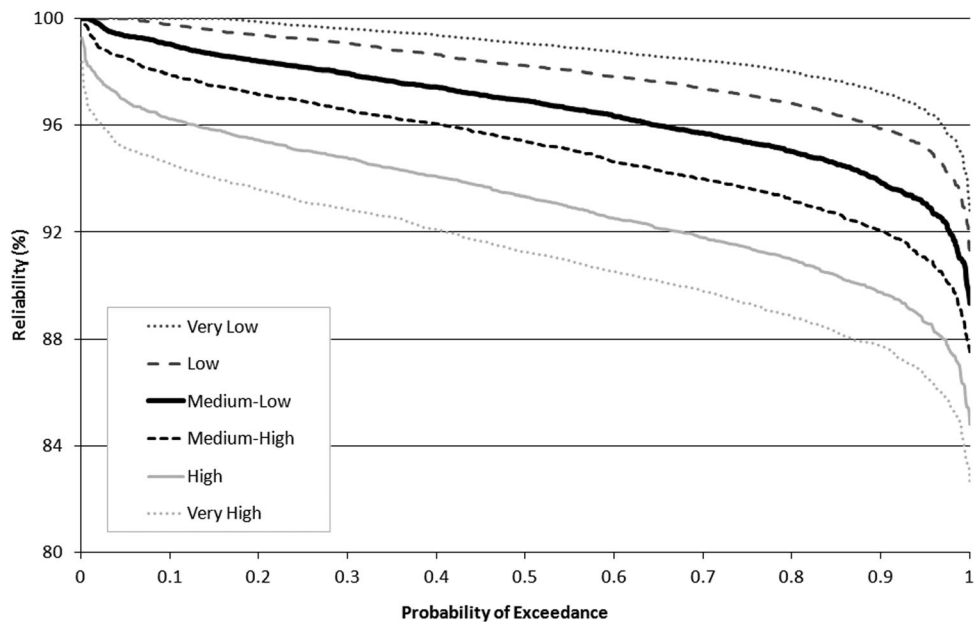


**Figure 6.** The cdf of reliability (based on 1000 stochastic rainfall time series) of Adelaide’s southern water supply system for different demands for 2020.

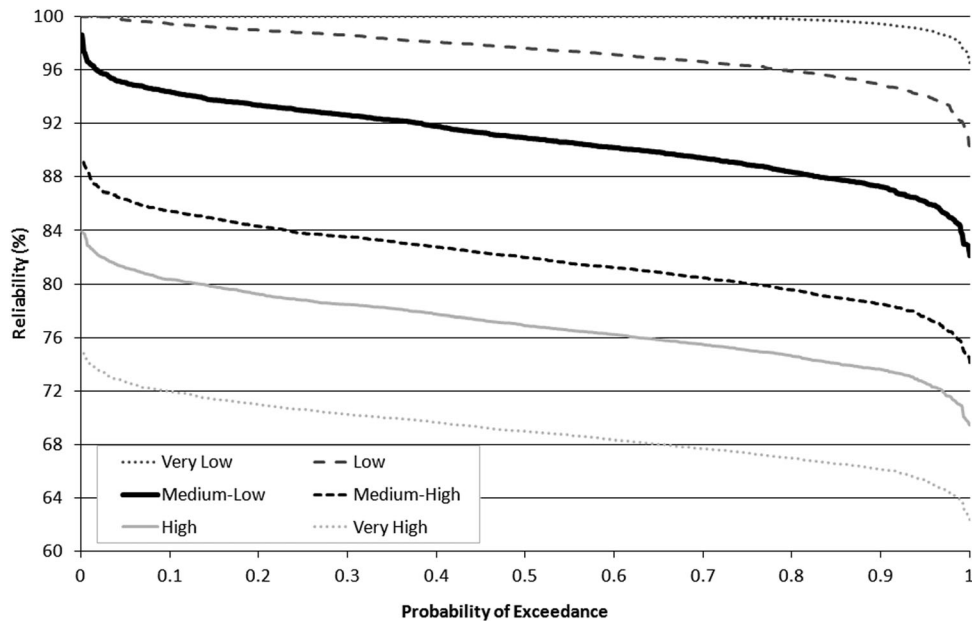


**Figure 7.** The cdf of reliability (based on 1000 stochastic rainfall time series) of Adelaide’s southern water supply system for different demands for 2050.

objective of the paper. The base case and scenarios 1–16 (Table 12) are analyzed in sections 4.1 and 4.2, while the average, best, and worst cases are analyzed in section 4.3.

**4.1. Relative Magnitudes of Sources of Uncertainty**

[69] In this section, the cdfs of the 1000 stochastic rainfall time series are illustrated for each of the 16 scenarios (Table 12) for 2020 and 2050 (Figures 3–7); for 2030 and 2040, median reliability values are illustrated in Figures 8–10 and 0.05 and 0.95 probabilities of exceedance values summarized in Table 13; while the cdf for natural rainfall variability for 2010 is illustrated in Figure 11. Cdfs of natural rainfall variability for the 16 scenarios for 2030 and 2040 are not illustrated, as the patterns were similar to those for 2020 and 2050 and the differences could be well illustrated in Table 13. Furthermore, the following discussion focuses on the median or 50th percentile values representing natural rainfall variability because the patterns between the scenarios are similar for all percentiles.

[70] The cdfs of reliability based on the 1000 stochastic rainfall time series of Adelaide’s southern water supply system for different SRES scenarios for 2020 and 2050 are shown in Figure 3. For the base case, the difference in median reliability across the SRES scenarios was 0.4% in 2020, which by 2050 had increased progressively to 2.0% (Figure 3 and Table 14). The order of SRES scenarios in terms of impact on reliability changed depending on the future year (Figure 3 and Table 13). By 2050, A1B returned greater reliabilities than A1FI and A1T, but smaller reliabilities than A2, B2, and B1 (Figure 3). While it was expected that B1 and B2 would produce more favorable reliabilities due to their more moderate development pathways (see section 3.4.1.1), it was not intuitive that A1T would produce the lowest reliabilities for 2020 and 2030, and the second lowest reliabilities in 2040 and 2050, because it represents the least fossil-fuel intensive pathway of the A1 family (see section 3.4.1.1). However, this can be

explained by examining the impacts of the development pathways in terms of changes to precipitation (sourced from OzClim for the FGOALS GCM) up until the end of the 21st century. A1FI has a greater impact on precipitation than A1T from 2040 onward, while A1B has a greater impact on precipitation than A1T from 2080 onward. Consequently, although by the end of the 21st century the impact on water supply security of A1FI and A1B should be greater than that of A1T, it did not occur for this case study due to the timeframe only extending to 2050.

**Table 13.** Probability of Exceedance Summary for Reliability for Years 2030 and 2040 for Each of the 16 Scenarios Detailed in Table 12

Uncertainty Source	Year	2030		2040		
		Probability of Exceedance	0.05	0.95	0.05	0.95
SRES scenario	B1		98.5	91.0	96.8	88.3
	B2		98.3	90.5	96.4	87.8
	A2		98.4	90.8	96.4	87.8
	A1B		98.3	90.5	96.2	87.6
	A1T		98.0	90.2	95.7	86.8
	A1FI		98.3	90.6	95.7	86.9
GCM	MIROC-m		98.3	90.7	96.4	87.9
	FGOALS		98.3	90.5	96.2	87.6
	CGCM-h		98.2	90.4	95.9	87.3
	MIROC-h		97.5	89.3	94.7	85.9
	MRI		96.0	87.4	92.6	83.2
	CCSM		95.3	86.3	91.4	81.9
Demand	CSIRO		87.1	78.1	79.7	72.3
	Very Low		100.0	97.5	100.0	98.2
	Low		100.0	94.8	99.7	94.0
	Medium-Low		98.3	90.5	96.2	87.6
	Medium-High		94.9	86.2	90.3	81.3
	High		91.5	82.4	85.4	76.5
	Very High		87.2	78.3	78.8	70.7

**Table 14.** Range in Median Reliability Caused by Uncertainty in SRES Scenario, GCM and Demand for 2020, 2030, 2040 and 2050 for Each of the 16 Scenarios in Table 12

Year	Uncertainty Source		
	SRES Scenario	GCM	Demand
2020	0.4	7.7	7.8
2030	0.6	12.5	16.8
2040	1.4	16.6	25.2
2050	2.0	20.0	31.0

[71] The cdfs of reliability (representing stochastic uncertainty in rainfall) of Adelaide's southern water supply system for different GCMs for 2020 and 2050 are illustrated in Figures 4 and 5, respectively. The difference in reliability across the GCMs was approximately 20 times that for the SRES scenarios in 2020, decreasing progressively to 10 times by 2050 (Figures 4 and 5). The lowest median reliability in 2050 was 71.5% under CSIRO (Figure 5). This was expected because the CSIRO GCM resulted in the greatest overall decrease in annual rainfall (23% reduction by 2050) compared to the other GCMs. Lower rainfall translated to Mount Bold storage levels being lower for longer periods, thus requiring water to be pumped from the River Murray for more days of the year, such that the annual River Murray license was used up earlier in the year and there were, therefore, more days of failure. MIROC-m and CGCM-h resulted in the greatest median reliabilities of 91.3% and 91.5% in 2050, respectively, which was expected considering these two GCMs resulted in very slight annual rainfall increases of 0.7% and 0.5% by 2050, respectively. Interestingly though, FGOALS with a 5.3% annual reduction in rainfall by 2050 only resulted in a slightly smaller median reliability of 90.9%, even though a similar reduction in annual rainfall was exhibited by CCSM (6.6% reduction by 2050), which returned reliabilities approximately 7% smaller than FGOALS (Figure 5). CCSM actually projected a smaller decrease in annual rainfall than MIROC-h (7.3%) and MRI (7.4%) but still returned a lower reliability. Furthermore, the similarity in annual rainfall reduction between MIROC-h and MRI was not translated into reliability with an approximate 4% difference between the two by 2050. These differences in the reliability patterns appear to be the result of differences in rainfall distribution over the year. Furthermore, these results illustrate both the complexity of studying the impacts of climate change on Adelaide's water supply security and the importance of considering seasonal variations for climate change scenarios.

[72] The cdfs of reliability based on natural rainfall variability of Adelaide's southern water supply system for different demand scenarios for 2020 and 2050 are shown in Figures 6 and 7, respectively. In a similar way to the SRES scenarios and GCMs, the range of water supply security increased with time across demand scenarios, so by 2050 reliability ranged from 69.0% for the very high demand scenario to 100% for the very low scenario (Figure 7). Thus, the range in median AAR of 31.0% across the demand scenarios was more than one and a half times that obtained across the seven GCMs and more than 15 times

that observed for the six SRES scenarios. The changes in reliability for each of the demand scenarios were to be expected, such that an increasing demand (due to a greater population and/or less water savings) resulted in a lower reliability (Figures 6 and 7).

[73] The six cdfs of natural climate variability (Figures 3–7) illustrate that reliability noticeably changed depending upon the particular stochastic rainfall time series. For example, for the base case, the difference between the minimum and maximum reliabilities was 10.7% in 2020, 12.9% in 2030, 15.5% in 2040, and 16.5% in 2050. This meant that demand uncertainty was always greater and SRES uncertainty always smaller than uncertainty due to natural rainfall variability, but compared to GCM uncertainty it was dependent on the future year; for 2020 and 2030, inherent natural rainfall variability created more uncertainty than GCMs, for 2040 the uncertainties were almost identical, and by 2050 GCMs were the second greatest source of uncertainty (Table 14). However, the extremely low probabilities of exceedance for reliability correspond to extremely large return periods (e.g., the maximum probability of exceedance is equivalent to 1 in 1000 year event), so these events are very unlikely. While this may appear to lessen the significance of the impact of natural rainfall variability, a 1 in 1000 year event is still possible. Second, as the probability of occurrence is unknown for each of the scenarios listed in Table 12, these scenarios could also be as unlikely to occur as a 1 in 1000 year event. Furthermore, when considering all scenarios in Table 12, natural rainfall variability can only cause up to 16%–17% variability at any of the years. This is because the greatest variation occurs when reliability ranges from 78% to 95% and this does not always occur for the base case. This pattern is believed to be a function of the large River Murray supply (65 GL/yr) that is, in this case study, unaffected by natural rainfall variability. In other words, when reliability is low (<78%–95%), the River Murray dominates supply, so natural variability in reservoir supply (reflecting natural rainfall variability) is dampened out by the climate-independent River Murray supply. However, when less River Murray supply is required, greater natural rainfall variability is expressed in the reliability, through reservoir supply. At very high reliabilities, the natural rainfall variability has less effect because there are fewer failures.

#### 4.1.1. Summary of Relative Magnitude of Uncertainty Sources

[74] For this case study, uncertainty source significance was dependent on the future year; however, demand was always the greatest source of uncertainty on water supply security and SRES scenario the least. Natural rainfall variability was second only to demand for the first half of the planning horizon, essentially equal to GCM uncertainty by 2040 and then of less importance than GCM choice by 2050. However, it is important to also remember that, while the synthetic rainfall data are believed to be representative of the historical 30-year time series they were derived from (section 3.2.6), this short time period may not reflect the real natural rainfall variability over a 100 year period. Therefore, natural rainfall variability could be underestimated in this analysis and could be an even greater source of uncertainty than determined here. These findings

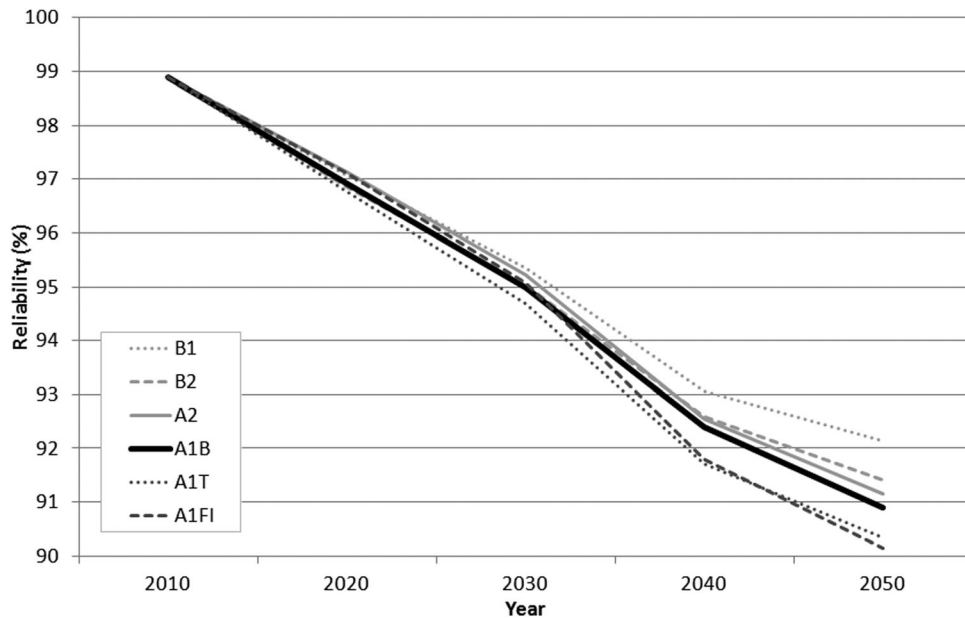


**Figure 8.** Change in median reliability over the planning horizon of Adelaide’s southern water supply system for different SRES scenarios.

indicate that, in analyzing the uncertainties of the impact of climate change on water supply systems, demand uncertainties, and natural rainfall variability, should not be excluded, as these can be greater sources of uncertainty than those associated with climate change modeling. They also illustrate the importance of analyzing changes in reliability progressively through time, such that if a longer planning horizon is selected, more effort can be directed to characterizing uncertainty of supply security due to demand and GCMs, while a shorter time period would suggest focus be directed on natural rainfall variability, as well as demand uncertainty.

[75] In terms of management implications, demand uncertainty could be reduced in the future by the water authority if they could control per capita consumption through demand management schemes and, while outside the scope of most water authorities, climate scientists working toward improving GCMs may also be able to reduce uncertainties associated with these model outputs. Of comfort to water authorities is the knowledge that the impact of SRES scenarios, in which uncertainty is irreducible, was minor compared to the other sources of uncertainty. Similarly, the planning of supply systems under demand uncertainty and natural rainfall variability is traditional for water

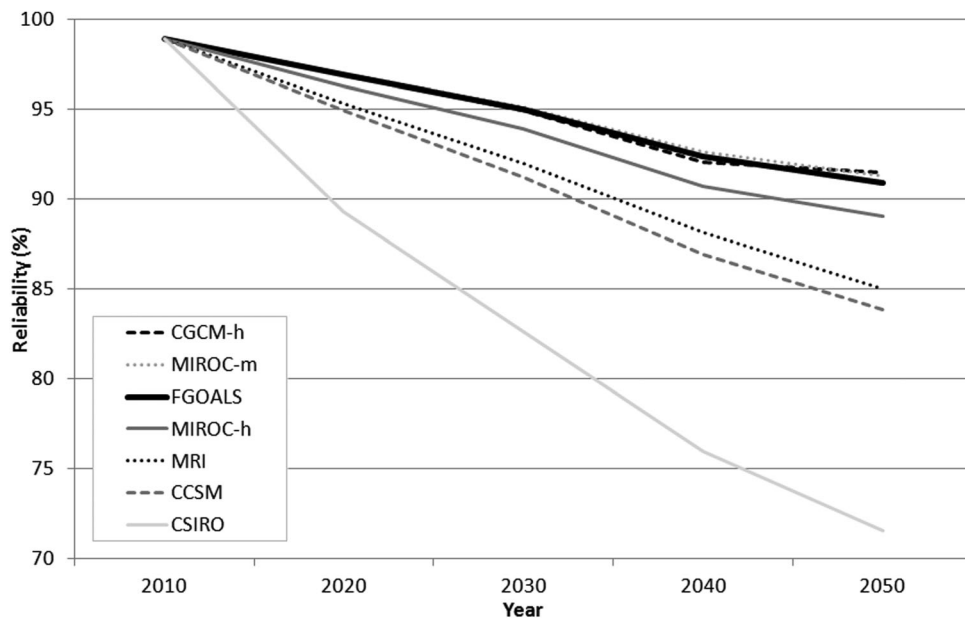


**Figure 9.** Change in median reliability over the planning horizon of Adelaide’s southern water supply system for different GCMs.

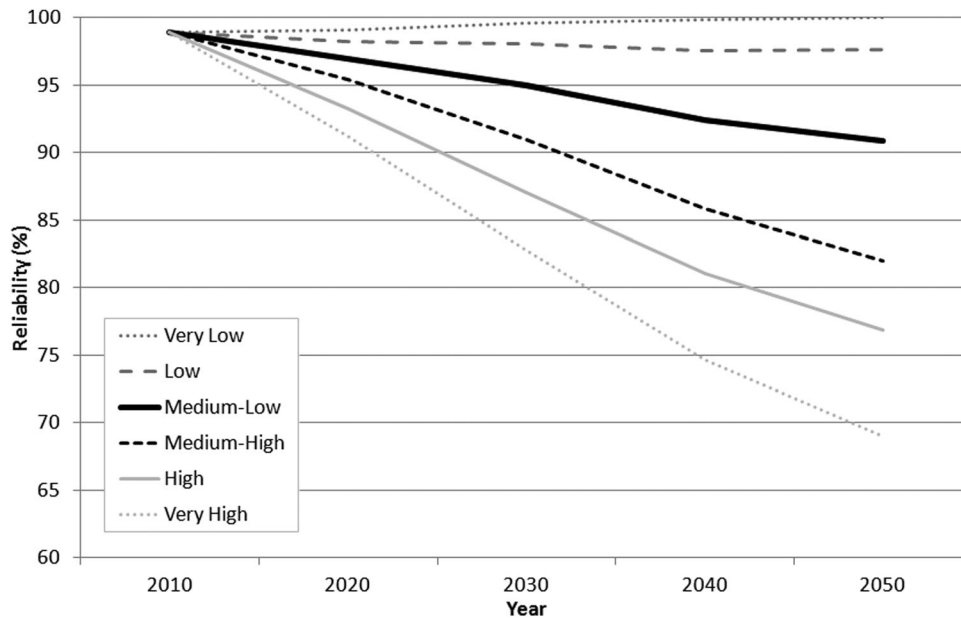


**Figure 10.** Change in median reliability over the planning horizon of Adelaide's southern water supply system for different demands.

authorities, so it is encouraging that these two sources were discovered to be the dominant sources of uncertainty, at least in the short term.

#### 4.2. Identifying Critical Points in Time for Water Supply Security

[76] Changes in median reliability of Adelaide's southern water supply system for different SRES scenarios are shown in Figure 8, while changes in median reliability for different GCMs are shown in Figure 9 and changes in median reliability for different demands are shown in Figure 10. Median reliability for the base case decreased from 98.9% in 2010 to 90.9% in 2050 (Figure 8), which was expected due to population growth and the increasingly adverse impacts of climate change. However, there was a good degree of variability in the trajectories of supply reliability over the planning horizon (Figures 8–10).

[77] As mentioned in section 1, understanding these changes in reliability with time, and their associated uncertainties, is important from a planning perspective, as additional supply sources or demand management schemes could be sequenced to come online when they are required to maintain reliability at an acceptable level. However, defining what an acceptable level is for reliability is subjective. While 100% reliability is desirable, when considering other objectives such as cost, water planners may accept a lower reliability for economic gain or accept the need for temporary water restrictions or other demand management actions. For example, if water supply planners accepted reliability levels in excess of 95%, then most of the 16 scenarios analyzed would at some stage over the planning horizon require supply to be increased or demand reduced. While this would occur around 2030 for the SRES scenarios (Figure 8); for the GCM scenarios, water supply security would be threatened between 2015 and 2030 (Figure 9); while for the demand scenarios, supply augmentation

or demand mitigation would be required between 2015 and 2030 or not at all (Figure 10).

[78] While the order of median reliability remained constant with time when comparing the different demand scenarios, the order of median reliability for the SRES scenarios and GCM scenarios changed slightly depending on the year (Figures 8 and 10). For example, A1FI resulted in a sharper decline in median reliability over the planning horizon than the other SRES scenarios, but this decline only accelerated after 2030 (Figure 8). Hence, the order of the impact of SRES scenarios and GCMs on water supply security is dependent on the year, which again highlights the importance of considering the temporal dimension when analyzing the impacts of climate change on water supply security.

[79] Over the planning horizon, the uncertainty in median reliability increased (Figures 8–10). While reliabilities were similar at the beginning of the planning horizon, the lowest median reliability for 2050 was 69.0% for the very high demand scenario, while the greatest median reliability was 100% for the very low demand scenario (Figure 10). Furthermore, differences in median reliability caused by the different sources of epistemic uncertainty were in agreement with the order of the magnitude of uncertainty sources defined in section 4.1 (without natural rainfall variability). A number of planning options, including the addition of alternative sources or demand management schemes could reduce this window of uncertainty in terms of water supply security; however, should the very low demand scenario ensue, then there would be a level of regret (for example unnecessary economic expenditure) associated with the selected option. Consequently, the findings illustrate that continual reassessment of planning may be necessary to ensure maximum reliability with minimal regret.

#### 4.3. Water Supply Security Ranges

[80] For the best case, Adelaide's southern supply system had slightly greater reliability in 2050 than in 2010,

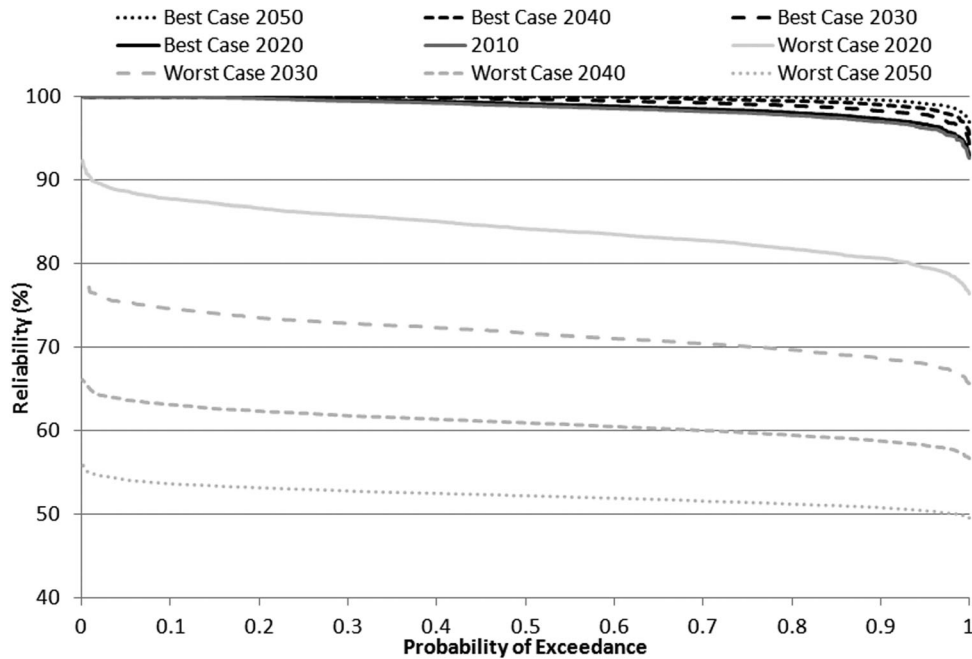


**Figure 11.** Cdf of reliability (based on 1000 stochastic rainfall time series) of Adelaide's southern water supply system for 2010 and for the Best and Worst Cases for 2020, 2030, 2040 and 2050.

which progressively increased with time over the planning horizon (Figure 11). While counterintuitive, this increase in reliability over time is caused by the very low demand scenario, which corresponds to a slight decrease in population and decreasing per capita consumption over the planning horizon (see section 3.4.1.1). If the best case ensued and water supply planners accepted reliability levels greater than 95%, then there is only a very slight probability that the supply system will not quite reach the target reliability in 2020 and 2030 due to natural rainfall variability, while for 2040 and 2050 it will always be met (Figure 11). In stark contrast, the worst case has reliabilities that decreased with time over the planning horizon and by 2050, for all stochastic rainfall time series, reliability was less than 56% (Figure 11). If 95% is considered the reliability threshold by the water authority and the worst case was to occur, then as early as 2020, the system would exhibit failures, regardless of natural rainfall variability. This stark contrast between the best and worst cases was expected, due to selecting SRES scenarios, GCMs, and demands that corresponded to the best and worst outcomes for reliability, respectively. As mentioned in section 4.2, the increasing uncertainty envelope with time was also expected, as projections made for the more distant future are less certain than those for the near future.

[81] The best and worst cases are both extreme cases and have low probabilities of occurrence. To place them in perspective, the average case was analyzed, which had a median reliability of 84% by 2050 (Figure 5), considerably smaller than the best case (100%), and much greater than the worst case (52%). However, while the best and worst cases are unlikely to occur, they do provide water authorities with the likely upper bound on the range of water supply security up to 2050. If some uncertainties can be reduced, which is likely in the future with projected

improvements to GCM model accuracy and potential demand management actions implemented by the water authority, then the overall uncertainty envelope will also be reduced. If the uncertainties are irreducible though, then the water authority must consider adaptation options that are extremely flexible, so as not to regret adaptation responses nor jeopardize water supply security. For example, if plans were made based on findings from the Worst case to ensure maximum water supply security and should the Best case occur, there would be a relatively high level of regret (such as unnecessary economic expenditure) associated with the selected option.

[82] These results from the best and worst cases also illustrate that the multiplicative impacts of epistemic uncertainty sources on supply reliability lessen the importance of natural rainfall variability. However, these cases are first not likely to occur and second, while the stochastic time series was found to preserve the important characteristics of the historical rainfall time series (section 3.2.6), the short 30 year historical rainfall time series may not have included the entire range of possible natural rainfall events, and so natural rainfall variability may be underestimated.

## 5. Summary and Conclusions

[83] Previous studies that have compared the magnitude of uncertainty sources associated with climate change impacts on water resources have largely focused on runoff. However, because of the nonlinear translation of runoff to water supply (due to a number of complexities in modeling water supply systems including the incorporation of demand and storages), there is a need to understand the importance of major uncertainty sources for climate change impacts on water supply security. Understanding the major sources of uncertainty and whether they are reducible or

not will help water authorities to focus efforts toward reducing uncertainty where possible or to develop strategies to cope with the uncertainties if they are irreducible. Furthermore, from a planning perspective, it is also important to understand changes in water supply security with time, and their associated uncertainties, so that additional supply sources or demand management schemes can be sequenced to come on line when they are required to raise water supply security to an acceptable level. This paper presents a scenario-based sensitivity approach for analyzing the impacts of climate change on water supply security tailored to the case study of Adelaide's southern water supply system. The methodology developed ensured that the three objectives of this paper were met, these being that (1) relative magnitudes of major sources of uncertainty on water supply security were assessed, (2) changes in water supply security through time were traced, and (3) water supply security ranges were established. Three major sources of systematic uncertainty—SRES scenarios, GCMs, and demand—were compared in the case study, as well as stochastic natural climate variability.

[84] In the earlier half of the adopted planning horizon of 2010–2050, the level of demand created the most uncertainty in water supply security, followed by natural rainfall variability, GCM, and lastly SRES scenario. By the later stages of the planning horizon though, GCMs created more uncertainty in reliability than natural rainfall variability. This suggests that, for studies analyzing the impacts of climate change on water supply security, uncertainties other than those associated with climate change and hydrological modeling should in fact be considered as they could have as great, or greater, impacts on water supply security projections. Furthermore, in the short term, efforts by water authorities should be directed toward demand and natural rainfall variability, but that for longer-term plans, uncertainties in GCMs should be analyzed.

[85] The case study also illustrated that reliability generally decreased over the planning horizon, a result of increasing demands and decreasing rainfall under climate change. From a local policy perspective, the projected reduction in system reliability realized in this analysis of Adelaide's southern system justifies (1) the production of flexible plans to ensure the security of Adelaide's future water supply and (2) the need for current and future initiatives to supplement Adelaide's water supply as well as curb demand.

[86] Furthermore, the findings illustrate the benefits from a water management perspective of assessing reliability progressively over a planning horizon to determine when to reduce demand and/or augment supply to maintain water supply security. However, the uncertainty envelope or range of uncertainty increased with time for Adelaide's southern system, which was particularly noticeable when comparing the best and worst cases. While some of this uncertainty may be reducible (by the water authority or others), stochastic uncertainty and some epistemic uncertainty will always exist, so flexible management may therefore be necessary to strike a balance between water supply security and regret. Thus a move away from single, long-lived, and large-scale centralized water sources toward decentralized, diverse water sources at much smaller scales is necessary [Pahl-Wostl, 2007]. For Adelaide's southern

system, this would mean that if supply were to be augmented by additional sources, local stormwater harvesting schemes or household rainwater tanks, would be preferred over centralized, larger-scale sources, such as a desalination plant. However, such climate-dependent sources have disadvantages compared with climate-independent sources (such as desalination), as climate-independent sources can guarantee supply (subject to loss of power and mechanical faults) regardless of whether it rains or not. Consequently, for Adelaide's southern system, trade-offs exist in selecting planning initiatives when attempting to maintain system reliability and minimize system regret. Future research should focus on identifying potential solutions for the southern system and the associated trade-offs.

[87] Furthermore, extending this research to examine multiple case studies and assess an increased number of uncertainty sources and scenarios would be valuable to determine whether generalized patterns and rules regarding the relative degree of uncertainty associated with particular major sources of uncertainty can be established. This would assist water planners in understanding where the greatest level(s) of effort should be focused when (1) attempting to reduce epistemic uncertainty and (2) developing tools to assist in planning for the future under great uncertainty. However, the findings of this case study clearly show that, in addition to examining demand uncertainty, natural rainfall variability must be considered in short-term plans, while in the longer-term, the focus will need to shift to consider the uncertainties of GCMs.

[88] **Acknowledgments.** This work is financed by The University of Adelaide and eWater CRC. We thank David Cresswell for his technical support of WaterCress and for adapting the program to suit the requirements of the case study. We also thank Sri Srikanthan for his assistance with SCL, Leanne Webb for running the CFF for this case study, Matthew Gibbs for his help with programming, Mark Thyer and Michael Leonard for their advice on catchment calibration, and the three anonymous reviewers who have assisted with improving the quality of this paper significantly.

## References

- Akaike, H. (1973), Information theory and an extension of the maximum likelihood principle, in *2nd International Symposium on Information Theory, Tsahkadsor, Armenia, USSR, September 2–8, 1971*, edited by B. Petrov and F. Csáki, pp. 267–281, Akadémiai Kiadó, Budapest.
- Alcorn, M. (2006), Surface water assessment of the currency creek catchment, Report DWLBC 2006/07, 61 pp., Dep. of Water, Land and Biodiversity Conservation, Adelaide, Australia.
- Australian Bureau of Statistics (2008), Population projections: Australia 2006 to 2101, Report, 96 pp., Australian Bureau of Statistics, Canberra.
- Barton, A. B. (2005), Management and reuse of local water resources in residential developments in Adelaide, 199 pp., Univ. of South Australia, Adelaide, Australia.
- Beven, K. (2006), A manifesto for the equifinality thesis, *J. Hydrol.*, 320(1–2), 18–36, doi:10.1016/j.jhydrol.2005.07.007.
- Boé, J., L. Terray, E. Martin, and F. Habets (2009), Projected changes in components of the hydrological cycle in French river basins during the 21st century, *Water Resour. Res.*, 45(8), W08426, doi:10.1029/2008WR007437.
- Bozdogan, H. (1987), Model selection and Akaike's Information Criterion (AIC): The general theory and its analytical extensions, *Psychometrika*, 52(3), 345–370, doi:10.1007/bf02294361.
- Charles, S. P., T. M. Heneker, and B. C. Bates (2008), Stochastically downscaled rainfall projections and modelled hydrological response for the Mount Lofty Ranges, South Australia, in *Proceedings of Water Down Under 2008*, edited by M. Lambert, T. Daniell, and M. Leonard, pp. 428–439, Engineers Australia; Casual Productions, Adelaide.



- Chen, J., F. P. Brissette, and R. Leconte (2011a), Uncertainty of downscaling method in quantifying the impact of climate change on hydrology, *J. Hydrol.*, 401(3–4), 190–202, doi:10.1016/j.jhydrol.2011.02.020.
- Chen, J., F. P. Brissette, A. Poulin, and R. Leconte (2011b), Overall uncertainty study of the hydrological impacts of climate change for a Canadian watershed, *Water Resour. Res.*, 47(12), W12509, doi:10.1029/2011WR010602.
- Chiew, F. H. S., and T. A. McMahon (2002), Modelling the impacts of climate change on Australian streamflow, *Hydrol. Process.*, 16, 1235–1245, doi:10.1002/hyp.1059.
- Chiew, F. H. S., and L. Siriwardena (2005), Trend: Trend/change detection software user guide, CRC for Catchment Hydrology, Australia.
- Chiew, F. H. S., D. G. C. Kirono, D. Kent, and J. Vaze (2009a), Assessment of rainfall simulations from global climate models and implications for climate change impact on runoff studies, in *18th World IMACS Congress and MODSIM09 International Congress on Modelling and Simulation*, edited by R. Anderssen, R. Braddock, and L. Newham, pp. 3907–3913, Modelling and Simulation Society of Australia and New Zealand and International Association for Mathematics and Computers in Simulation, Canberra.
- Chiew, F. H. S., J. Teng, J. Vaze, and D. G. C. Kirono (2009b), Influence of global climate model selection on runoff impact assessment, *J. Hydrol.*, 379(1–2), 172–180, doi:10.1016/j.jhydrol.2009.10.004.
- Chiew, F. H. S., J. Teng, J. Vaze, D. A. Post, J. M. Perraud, D. G. C. Kirono, and N. R. Viney (2009c), Estimating climate change impact on runoff across southeast Australia: Method, results, and implications of the modeling method, *Water Resour. Res.*, 45(10), W10414, doi:10.1029/2008WR007338.
- Chiew, F. H. S., D. G. C. Kirono, D. M. Kent, A. J. Frost, S. P. Charles, B. Timbal, K. C. Nguyen, and G. Fu (2010), Comparison of runoff modelled using rainfall from different downscaling methods for historical and future climates, *J. Hydrol.*, 387(1–2), 10–23, doi:10.1016/j.jhydrol.2010.03.025.
- Clarke, J. M., P. H. Whetton, and K. J. Hennessy (2011), Providing application-specific climate projections datasets: CSIRO's Climate Futures Framework, in *MODSIM2011, 19th International Congress on Modelling and Simulation*, edited by F. Chan, D. Marinova, and R. Anderssen, pp. 2683–2690, Modelling and Simulation Society of Australia and New Zealand, Canberra.
- Crawley, P. D. (1995), *Risk and Reliability Assessment of Multiple Reservoir Water Supply Headworks Systems*, 601 pp., Univ. of Adelaide, Adelaide.
- Crawley, P. D., and G. C. Dandy (1993), Optimal operation of multiple-reservoir system, *J. Water Resour. Plann. Manage.*, 119(1), 1–17, doi:10.1061/(ASCE)0733-9496(1993)119:1(1).
- Cubasch, U., G. A. Meehl, G. J. Boer, R. J. Stouffer, M. Dix, A. Noda, C. A. Senior, S. Raper, and K. S. Yap (2001), Projections of future climate change, in *Climate Change 2001: The Scientific Basis. Contribution of Working Group I to the Third Assessment Report of the Intergovernmental Panel on Climate Change*, edited by J. T. Houghton et al., p. 881, Cambridge Univ. Press, Cambridge, U. K.
- Diaz-Nieto, J., and R. L. Wilby (2005), A comparison of statistical downscaling and climate change factor methods: Impacts on low flows in the River Thames, United Kingdom, *Clim. Change*, 69(2), 245–268, doi:10.1007/s10584-005-1157-6.
- Dibike, Y. B., and P. Coulibaly (2005), Hydrologic impact of climate change in the Saguenay watershed: Comparison of downscaling methods and hydrologic models, *J. Hydrol.*, 307(1–4), 145–163, doi:10.1016/j.jhydrol.2004.10.012.
- Forbes, K., S. Kienzle, C. Coburn, J. Byrne, and J. Rasmussen (2011), Simulating the hydrological response to predicted climate change on a watershed in southern Alberta, Canada, *Clim. Change*, 105(3), 555–576, doi:10.1007/s10584-010-9890-x.
- Fowler, H. J., C. G. Kilsby, and P. E. O'Connell (2003), Modeling the impacts of climatic change and variability on the reliability, resilience, and vulnerability of a water resource system, *Water Resour. Res.*, 39(8), 11, doi:10.1029/2002WR001778.
- Fowler, H. J., S. Blenkinsop, and C. Tebaldi (2007), Linking climate change modelling to impacts studies: Recent advances in downscaling techniques for hydrological modelling, *Int. J. Climatol.*, 27(2), 1547–1578, doi:10.1002/joc.1556.
- Gober, P., C. W. Kirkwood, R. C. Balling, A. W. Ellis, and S. Deitrick (2010), Water planning under climatic uncertainty in Phoenix: Why we need a new paradigm, *Ann. Assoc. Am. Geogr.*, 100(2), 356–372, doi:10.1080/00045601003595420.
- Government of South Australia (2005), *Water Proofing Adelaide—A Thirst for Change 2005–2025*, 60 pp., Gov. of South Australia, Adelaide, Australia.
- Government of South Australia (2009), *Water for Good—A Plan to Ensure Our Water Future to 2050*, 190 pp., Gov. of South Australia, Adelaide, Australia.
- Groves, D. G., D. Yates, and C. Tebaldi (2008), Developing and applying uncertain climate change projections for regional water management planning, *Water Resour. Res.*, 44(12), W12413, doi:10.1029/2008WR006964.
- House-Peters, L. A., and H. Chang (2011), Urban water demand modeling: Review of concepts, methods, and organizing principles, *Water Resour. Res.*, 47, W05401, doi:10.1029/2010WR009624.
- Intergovernmental Panel on Climate Change (2000), Special report on emissions scenarios, 570 pp., Cambridge Univ. Press, U.K.
- Intergovernmental Panel on Climate Change (2007), Climate change 2007: Synthesis report. Contribution of Working Groups I, II and III to the Fourth Assessment Report of the Intergovernmental Panel on Climate Change, 104 pp., IPCC, Geneva, Switzerland.
- Irving, D. B., et al. (2011), Evaluating global climate models for the Pacific island region, *Clim. Res.*, 49(3), 169–187, doi:10.3354/cr01028.
- Jain, S. K., and K. P. Sudheer (2008), Fitting of hydrologic models: A close look at the Nash–Sutcliffe index, *J. Hydrol. Eng.*, 13(10), 981–986, doi:10.1061/(asce)1084-0699(2008)13:10(981).
- Jeffrey, S. J., J. O. Carter, K. B. Moodie, and A. R. Beswick (2001), Using spatial interpolation to construct a comprehensive archive of Australian climate data, *Environ. Modell. Software*, 16(4), 309–330, doi:10.1016/S1364-8152(01)00008-1.
- Kaczmarek, Z., J. Napiorkowski, and M. Strzepek (1996), Climate change impacts on the water supply system in the Warta River catchment, Poland, *Water Resour. Dev.*, 12(2), 165–180, doi:10.1080/07900629650041939.
- Kilsby, C. G., P. D. Jones, A. Burton, A. C. Ford, H. J. Fowler, C. Harpham, P. James, A. Smith, and R. L. Wilby (2007), A daily weather generator for use in climate change studies, *Environ. Modell. Software*, 22(12), 1705–1719, doi:10.1016/j.envsoft.2007.02.005.
- Lopez, A., F. Fung, M. New, G. Watts, A. Weston, and R. L. Wilby (2009), From climate model ensembles to climate change impacts and adaptation: A case study of water resource management in the southwest of England, *Water Resour. Res.*, 45(8), W08419, doi:10.1029/2008WR007499.
- Majone, B., C. I. Bovolo, A. Bellin, S. Blenkinsop, and H. J. Fowler (2012), Modeling the impacts of future climate change on water resources for the Gállego river basin (Spain), *Water Resour. Res.*, 48(1), W01512, doi:10.1029/2011WR010985.
- Manning, L. J., J. W. Hall, H. J. Fowler, C. G. Kilsby, and C. Tebaldi (2009), Using probabilistic climate change information from a multimodel ensemble for water resources assessment, *Water Resour. Res.*, 45(11), W11411, doi:10.1029/2007WR006674.
- Milly, P. C. D., J. Betancourt, M. Falkenmark, R. M. Hirsch, Z. W. Kundzewicz, D. P. Lettenmaier, and R. J. Stouffer (2008), Climate change—Stationarity is dead: Whither water management?, *Science*, 319(5863), 573–574, doi:10.1126/science.1151915.
- Moriassi, D. N., J. G. Arnold, M. W. Van Liew, R. L. Bingner, R. D. Harmel, and T. L. Veith (2007), Model evaluation guidelines for systematic quantification of accuracy in watershed simulations, *Am. Soc. Agric. Biol. Eng.*, 50(3), 885–900.
- Morton, F. I. (1983), Operational estimates of areal evapotranspiration and their significance to the science and practice of hydrology, *J. Hydrol.*, 66(1–4), 1–76, doi:10.1016/0022-1694(83)90177-4.
- Mpelasoka, F. S., and F. H. S. Chiew (2009), Influence of rainfall scenario construction methods on runoff projections, *J. Hydrometeorol.*, 10(5), 1168–1183, doi:10.1175/2009jhm1045.1.
- O'Hara, J., and K. Georgakakos (2008), Quantifying the urban water supply impacts of climate change, *Water Resour. Manage.*, 22(10), 1477–1497, doi:10.1007/s11269-008-9238-8.
- Pahl-Wostl, C. (2007), Transitions towards adaptive management of water facing climate and global change, *Water Resour. Manage.*, 21(1), 49–62, doi:10.1007/s11269-006-9040-4.
- Perkins, S. E., and A. J. Pitman (2009), Do weak AR4 models bias projections of future climate changes over Australia?, *Clim. Change*, 93(3–4), 527–558, doi:10.1007/s10584-008-9502-1.
- Randall, D. A., et al. (2007), Climate models and their evaluation, in *Climate Change 2007: The Physical Science Basis. Contribution of Working Group I to the Fourth Assessment Report of the Intergovernmental*

- Panel on Climate Change*, edited by S. Solomon, et al., pp. 589–662, Cambridge Univ. Press, Cambridge, U. K.
- Rayner, D. (2005), Australian synthetic daily Class A pan evaporation, Report QNRM05435, 38 pp., Dep. of Nat. Resources and Mines, Queensland, Brisbane.
- Refsgaard, J. C., and B. Storm (1996), Construction, calibration and validation of hydrological models, in *Distributed Hydrological Modelling*, edited by M. B. Abbott and J. C. Refsgaard, pp. 41–54., Kluwer Acad., Dordrecht, Netherlands.
- Salas, J., B. Rajagopalan, L. Saito, and C. Brown (2012), Special section on climate change and water resources: Climate nonstationarity and water resources management, *J. Water Resour. Plann. Manage.*, 138(5), 385–388, doi:10.1061/(ASCE)WR.1943-5452.0000279.
- Savadamuthu, K. (2003), Surface water assessment of the Upper Finnis Catchment, Report DWLBC 2003/18, Dep. of Water, Land and Biodiversity Conservation, Adelaide, Australia.
- Schoups, G., N. C. van de Giesen, and H. H. G. Savenije (2008), Model complexity control for hydrologic prediction, *Water Resour. Res.*, 44, W00B03, doi:10.1029/2008WR006836.
- Singh, J., H. V. Knapp, and M. Demissie (2004), Hydrologic modelling of the Iroquois River watershed using HSPF and SWAT, Report ISWS CR 2004-08, 24 pp., Watershed Science Section, Illinois State Water Survey, Champaign.
- Srikanthan, R. (2005), Stochastic generation of daily rainfall at a number of sites, Report 05/7, CRC for Catchment Hydrology, Canberra.
- Srikanthan, R., and T. A. McMahon (2001), Stochastic generation of annual, monthly and daily climate data: A review, *Hydrol. Earth Syst. Sci.*, 5(4), 653–670.
- Srikanthan, R., and G. G. S. Pegram (2009), A nested multisite daily rainfall stochastic generation model, *J. Hydrol.*, 371(1–4), 142–153, doi:10.1016/j.jhydrol.2009.03.025.
- Srikanthan, R., F. H. S. Chiew, and A. J. Frost (2004), *SCL: Stochastic Climate Library User Guide*, CRC for Catchment Hydrology, Canberra.
- Teoh, K. S. (2002), *Estimating the Impact of Current Farm Dams Development on the Surface Water Resources of the Onkaparinga River Catchment*, 153 pp., The Dep. of Water, Land and Biodiversity Conservation, Adelaide, Australia.
- Traynham, L., R. Palmer, and A. Polebitski (2011), Impacts of future climate conditions and forecasted population growth on water supply systems in the Puget Sound Region, *J. Water Resour. Plann. Manage.*, 137(4), 318–326, doi:10.1061/(asce)wr.1943-5452.0000114.
- van Oldenborgh, G. J., S. Philip, and M. Collins (2005), El Nino in a changing climate: A multi-model study, *Ocean Sci. Discuss.*, 2(3), 267–298.
- Vicuna, S., J. A. Dracup, J. R. Lund, L. L. Dale, and E. P. Maurer (2010), Basin-scale water system operations with uncertain future climate conditions: Methodology and case studies, *Water Resour. Res.*, 46(4), W04505, doi:10.1029/2009WR007838.
- Wagener, T., H. S. Wheater, and H. V. Gupta (2004), *Rainfall-Runoff Modelling in Gauged and Ungauged Catchments*, 306 pp., Imperial College Press, London.
- Wang, Q. J. (1991), The genetic algorithm and its application to calibrating conceptual rainfall-runoff models, *Water Resour. Res.*, 27(9), 2467–2471, doi:10.1029/91WR01305.
- Whetton, P., K. Hennessy, J. Clarke, K. McInnes, and D. Kent (2012), Use of representative climate futures in impact and adaptation assessment, *Clim. Change*, 1–10, doi:10.1007/s10584-012-0471-z.
- Wilby, R. L., and S. Dessai (2010), Robust adaptation to climate change, *Weather*, 65(7), 180–185, doi:10.1002/wea.543.
- Wilby, R. L., and H. J. Fowler (2011), Regional climate downscaling, in *Modelling the Impact of Climate Change on Water Resources*, edited by F. Fung, A. Lopez, and M. New, pp. 34–85, Blackwell, Oxford.
- Wilby, R. L., and I. Harris (2006), A framework for assessing uncertainties in climate change impacts: Low-flow scenarios for the River Thames, UK, *Water Resour. Res.*, 42(2), W02419, doi:10.1029/2005WR004065.
- Wilby, R. L., P. G. Whitehead, A. J. Wade, D. Butterfield, R. J. Davis, and G. Watts (2006), Integrated modelling of climate change impacts on water resources and quality in a lowland catchment: River Kennet, UK, *J. Hydrol.*, 330(1–2), 204–220, doi:10.1016/j.jhydrol.2006.04.033.
- Wiley, M. W., and R. N. Palmer (2008), Estimating the impacts and uncertainty of climate change on a municipal water supply system, *J. Water Resour. Plann. Manage.*, 134(3), 239–246, doi:10.1061/(asce)0733-9496(2008)134:3(239).
- Zhu, T., M. W. Jenkins, and J. R. Lund (2005), Estimated impacts of climate warming on California water availability under twelve future climate scenarios, *J. Am. Water Resour. Assoc.*, 41(5), 1027–1038, doi:10.1111/j.1752-1688.2005.tb03783.x.